

**A critical review by Dr Martin Elsner of the Institute of Groundwater Ecology, Helmholtz Zentrum München.**

**Title: Stable isotope fractionation to investigate natural transformation mechanisms of organic contaminants: principles, prospects and limitations**

Compound specific isotope studies have the unique potential to elucidate transformation mechanisms of organic pollutants (*i.e.*, the manner and order of chemical bond cleavage) directly in the environment.

**As featured in:**



See Elsner, *J. Environ. Monit.*, 2010, **12**, 2005–2031

**RSC Publishing**

**www.rsc.org**

Registered Charity Number 207890

# Stable isotope fractionation to investigate natural transformation mechanisms of organic contaminants: principles, prospects and limitations†

Martin Elsner

Received 8th June 2010, Accepted 27th August 2010

DOI: 10.1039/c0em00277a

Gas chromatography–isotope ratio mass spectrometry (GC-IRMS) has made it possible to analyze natural stable isotope ratios (*e.g.*,  $^{13}\text{C}/^{12}\text{C}$ ,  $^{15}\text{N}/^{14}\text{N}$ ,  $^2\text{H}/^1\text{H}$ ) of individual organic contaminants in environmental samples. They may be used as fingerprints to infer contamination sources, and may demonstrate, and even quantify, the occurrence of natural contaminant transformation by the enrichment of heavy isotopes that arises from degradation-induced isotope fractionation. This review highlights an additional powerful feature of stable isotope fractionation: the study of environmental transformation mechanisms. Isotope effects reflect the energy difference of isotopologues (*i.e.*, molecules carrying a light *versus* a heavy isotope in a particular molecular position) when moving from reactant to transition state. Measuring isotope fractionation, therefore, essentially allows a glimpse at transition states! It is shown how such position-specific isotope effects are “diluted out” in the compound average measured by GC-IRMS, and how a careful evaluation in mechanistic scenarios and by dual isotope plots can recover the underlying mechanistic information. The mathematical framework for multistep isotope fractionation in environmental transformations is reviewed. Case studies demonstrate how isotope fractionation changes in the presence of mass transfer, enzymatic commitment to catalysis, multiple chemical reaction steps or limited bioavailability, and how this gives information about the individual process steps. Finally, it is discussed how isotope ratios of individual products evolve in sequential or parallel transformations, and what mechanistic insight they contain. A concluding session gives an outlook on current developments, future research directions and the potential for bridging the gap between laboratory and real world systems.

## Introduction

Monitoring of organic contaminants in the environment has continuously been advanced by the development of new analytical approaches. In many cases, detection and quantification of single organic substances in complex environmental samples would not be possible without separation by gas chromatography (GC) or liquid chromatography (LC). Structural information has been accessible through coupling to (tandem) mass spectrometry (GC-MS, LC-MS/MS). The recent hyphenation *via* combustion or pyrolysis ovens to dedicated isotope ratio mass spectrometers (GC-IRMS, LC-IRMS) now makes it possible to

analyze even precise natural isotope ratios ( $^{13}\text{C}/^{12}\text{C}$ ,  $^{15}\text{N}/^{14}\text{N}$ ,  $^2\text{H}/^1\text{H}$ ) of organic contaminants in environmental samples.<sup>1–3</sup>

An immediate result of such methodological advances is the possibility to establish inventories of environmental contamination: What compounds are detected in drinking water wells? What are their concentrations? Can isotope ratios be used as fingerprints to identify the liable party of a groundwater contamination? While such monitoring is essential to establish inventories of pollution, long-term impacts can only be predicted if the natural attenuation reactions are understood that lead to contaminant elimination. In this context, an important consequence of a new analytical method development is also the possibility to learn more about the *processes* that organic compounds undergo in natural systems.

GC-MS can deliver measurements of volatile organic compounds and their decrease in concentrations. Such

*Institute of Groundwater Ecology, Helmholtz Zentrum München - German Research Center for Environmental Health, Ingolstädter Landstr. 1, 85764 Neuherberg, Germany. E-mail: martin.elsner@helmholtz-muenchen.de*

† Published as part of a special issue dedicated to Emerging Investigators.

## Environmental impact

To predict the long-term impact of organic contaminants, transformation mechanisms that lead to their elimination need to be understood. Studies in the field are generally limited to the monitoring of compound concentrations, whereas mechanistic studies in the laboratory face the difficulty of transferring insight into real world systems. Compound-specific isotope fractionation studies bear the unique potential to bridge this gap: measurable changes in contaminant isotope ratios may be linked to kinetic isotope effects, which, in turn, reflect the transition state structure of the underlying (bio)chemical transformation reactions. Mechanistic insight becomes, therefore, accessible directly in natural systems! This critical review discusses the fundamentals and recent developments in this young, emerging research area and gives an outlook on prospects and limitations of future studies.

dissipation kinetics alone, however, cannot distinguish true compound elimination as opposed to dilution or sorption. LC-MS/MS allows in addition analysis of polar degradation products and metabolites. This insight is more conclusive, but may fail again if products are quickly further metabolized so that they are not accessible to analysis. Even when contaminants and their products can both be detected, only net degradation pathways can be established. What are the underlying transformation mechanisms? What is the strategy of microorganisms on the enzymatic level to break down contaminants that are difficult to deal with? To answer these questions, an analytical approach is required that allows the analysis of not only reactants and products, but essentially transition states of biochemical transformations. This critical review focuses on the measurement of stable isotope fractionation *via* GC-IRMS as a new conceptual advance that can for the first time provide this quality of information. It will not deal with the fundamentals of compound-specific isotope analysis itself which have been treated elsewhere in excellent reviews.<sup>1–3</sup> Instead the focus of this review will be on the interpretation of compound-specific isotope data: What can stable isotope fractionation measurements tell us? What are the underlying processes? What are the prospects and limitations for interpretations?

In a first part it is discussed how the enrichment of heavy isotopes inside an organic contaminant can detect, and even quantify, natural transformation at contaminated groundwater sites, even in the absence of mass balances. A second part highlights that this isotopic enrichment reflects underlying kinetic isotope effects. Since these depend on the transition state structure of the associated transformations it is shown how observable isotope fractionation may be linked to different transformation mechanisms. A third part critically discusses that isotope fractionation in multistep processes may depend on several process steps and considers the implications for interpretations. In a fourth part the importance of product formation for observable isotope fractionation is discussed. A concluding section presents current developments and future research directions.



Martin Elsner

*Martin Elsner received his Diploma and his PhD from ETH Zürich, Switzerland. He became fascinated by stable isotope studies when conducting his PhD with Prof. René Schwarzenbach and Prof. Stefan Haderlein at EAWAG, and subsequently, working for two years as a DFG postdoctoral fellow with Prof. Barbara Sherwood Lollar at the University of Toronto, Canada. In January 2006 he became Helmholtz Junior Research Group Leader in the Institute of*

*Helmholtz Zentrum München, Germany. His research group uses stable isotope fractionation to study environmental transformation reactions of organic contaminants, with a particular focus on pesticides and chlorinated hydrocarbons.*

## I. Practical use of isotopes to monitor groundwater contamination

**Isotopes as reactive probes to demonstrate the occurrence of contaminant degradation.** For the monitoring of groundwater contaminations, the most immediate added values of compound-specific isotope analysis by GC-IRMS have been (i) the possibility of isotopic fingerprinting to distinguish contamination sources<sup>4–7</sup> and (ii) the ability to demonstrate the occurrence of natural transformation reactions. The latter aspect is of particular interest in the management of contaminated sites. Legislation requires a direct line of evidence of Natural Attenuation,<sup>8</sup> but characterization of the subsurface is often difficult, installation of monitoring wells is expensive, and mass balances are difficult to close. Independent means are therefore needed to demonstrate with a reasonable number of sampling wells that organic contaminants are naturally broken down.

Such an additional line of evidence can be provided by measurements of the isotope values of organic contaminants in groundwater samples, for example for carbon isotopes (<sup>13</sup>C, <sup>12</sup>C):

$$\delta^{13}\text{C}_{\text{compound}} = \frac{\left(\frac{^{13}\text{C}}{^{12}\text{C}}\right)_{\text{compound}} - \left(\frac{^{13}\text{C}}{^{12}\text{C}}\right)_{\text{ref}}}{\left(\frac{^{13}\text{C}}{^{12}\text{C}}\right)_{\text{ref}}} = \frac{\left(\frac{^{13}\text{C}}{^{12}\text{C}}\right)_{\text{compound}}}{\left(\frac{^{13}\text{C}}{^{12}\text{C}}\right)_{\text{ref}}} - 1 \quad (1)$$

Here, (<sup>13</sup>C/<sup>12</sup>C)<sub>compound</sub> is the isotope ratio of the organic compound, (<sup>13</sup>C/<sup>12</sup>C)<sub>ref</sub> is the isotope ratio of the international reference material (V-PDB, Vienna Pee Dee Belemnite for carbon) and δ<sup>13</sup>C<sub>compound</sub> is the reported isotope value. Expressing isotope values in this Delta notation has two advantages. (1) Values are recorded relative to a common international reference so that measurements of different laboratories are comparable on an absolute scale. (2) Absolute values would give awkward numbers (e.g., (<sup>13</sup>C/<sup>12</sup>C)<sub>ref</sub> = 0.0111799),<sup>9</sup> whereas differences are easier to work with. δ<sup>13</sup>C<sub>compound</sub> = −0.011 = −11‰, for example, immediately indicates that an organic compound contains 0.011 times less <sup>13</sup>C per <sup>12</sup>C than the international reference material, corresponding to −1.1%, or −11‰. To put this into perspective, the typical error of GC-IRMS measurements is ±0.5‰ for carbon, ±1‰ for nitrogen and ±5‰ for hydrogen.<sup>3,10</sup> Traditionally, expressions like eqn (1) contain a factor of 1000 so that numbers like “−0.011” are converted to read “−11”. However, since −0.011 is exactly equal to −11‰, such a conversion is not needed and may lead to misunderstandings. This convention is being discouraged by the latest IUPAC convention<sup>11</sup> and will not be used in this review.

To obtain proof that a contaminant is degraded at a contaminated site, one makes use of the kinetic isotope effect associated with chemical and biochemical reactions. Typically, chemical bonds are broken more easily if they contain a light rather than a heavy isotope.<sup>12</sup> Organic contaminant molecules with heavy isotopes are therefore degraded more slowly and tend to accumulate in the fraction of molecules that remain when natural transformation occurs. Such an enrichment of heavy isotopes can be measured as more positive isotope values in the Delta notation when the contaminant is analyzed *via* GC-IRMS. If a contaminant sample downstream of a suspected source area

shows such isotopic enrichment, this therefore gives a strong line of evidence that natural attenuation occurs<sup>13</sup> – even when mass balances cannot be closed and metabolites are not detected!

In this context it is frequently assumed that processes of physical nature (*i.e.*, diffusion, sorption, volatilization) are associated with much smaller isotope fractionation that is generally neglected. These aspects are discussed in more detail by Hunkeler and Elsner.<sup>14</sup> The current view is that in aquifers, under saturated conditions and with contaminant plumes at steady state, these processes are indeed negligible.<sup>15</sup> Possible exceptions are contaminant plumes at non-steady state where transverse dispersion<sup>16,17</sup> and sorption<sup>18,19</sup> may create small transient isotope gradients even in the absence of degradation. For the unsaturated zone, even greater isotope gradients may transiently arise by diffusion,<sup>20</sup> while isotope effects during volatilization tend to play a minor role.<sup>20,21</sup>

**Quantitative estimates of natural degradation from isotope measurements.** Contaminant-specific isotope measurements do not only offer the possibility to *qualitatively detect*, but also to *quantitatively estimate the extent* of contaminant degradation. Since transformation causes isotope fractionation, greater changes in isotope values are expected for a greater extent of degradation. What is needed is an equation that links degradation-induced shifts in isotope ratios to the extent of degradation by which they have been caused. Such a relationship is given by the Rayleigh equation,<sup>22,23</sup> for example for carbon isotopes:

$$\frac{(^{13}\text{C}/^{12}\text{C})}{(^{13}\text{C}/^{12}\text{C})_0} = \frac{\delta^{13}\text{C} + 1}{\delta^{13}\text{C}_0 + 1} = f^{(\alpha-1)} = f^\varepsilon \quad (2)$$

Here,  $(^{13}\text{C}/^{12}\text{C})_0$  is the carbon isotope ratio of a given organic compound when it has not yet been degraded.  $(^{13}\text{C}/^{12}\text{C})$  is the isotope ratio of the same compound after a certain extent of degradation has occurred, and  $f$  is the fraction of the compound remaining at this stage of degradation.  $\delta^{13}\text{C}_0$  and  $\delta^{13}\text{C}$  are the isotope ratios expressed in the Delta notation. Isotope values and  $f$  are linked by the fractionation factor  $\alpha$  (or enrichment factor  $\varepsilon$ ) which may be evaluated from experimental data in a double logarithmic plot:

$$\ln\left(\frac{\delta^{13}\text{C} + 1}{\delta^{13}\text{C}_0 + 1}\right) = (\alpha - 1) \cdot \ln f = \varepsilon \cdot \ln f \quad (3)$$

Such numbers of  $\alpha$  and  $\varepsilon$  may be determined in laboratory experiments with aquifer sediments or microbial cultures mimicking the conditions expected under natural conditions, or they may be looked up in the literature.<sup>24–27</sup> Subsequently, isotope values close to a contaminant source ( $\delta^{13}\text{C}_0$ ) and further downstream in a contaminated aquifer ( $\delta^{13}\text{C}$ ) may be used to estimate the extent of (bio)degradation  $B$  on the flow path between the two sampling points according to

$$\begin{aligned} B &= (1 - f) = 1 - \left(\frac{\delta^{13}\text{C} + 1}{\delta^{13}\text{C}_0 + 1}\right)^{1/(\alpha-1)} \\ &= 1 - \left(\frac{\delta^{13}\text{C} + 1}{\delta^{13}\text{C}_0 + 1}\right)^{1/\varepsilon} \end{aligned} \quad (4)$$

Alternatively, changes in isotope ratios may be measured over time at a given monitoring well to investigate the efficiency of an

ongoing *in situ* remediation scheme. As discussed in recent reviews,<sup>6,24,28</sup> the feasibility of this approach has been successfully demonstrated at numerous field sites contaminated with fuel oxygenates,<sup>29–32</sup> chlorinated hydrocarbons,<sup>13,33–40</sup> petroleum hydrocarbons<sup>41–46</sup> or RDX.<sup>47</sup> Official guidelines have been published which recommend the use of stable isotope fractionation measurements to estimate the extent of biodegradation at contaminated sites.<sup>26,48,49</sup>

Current research is now concentrating on the uncertainties associated with such estimates. One uncertainty is related to the value of  $\alpha$ , or  $\varepsilon$ , respectively. Are values reported in the literature applicable to a specific field site? How robust or variable are such numbers of  $\varepsilon$ ? What are the underlying factors that determine their magnitude? These aspects will be considered in detail in this review. Another uncertainty arises by the fact that water parcels travelling in an aquifer are not closed reaction vessels like in the laboratory. Instead, contaminants are subject to sorption, volatilization or mixing through dispersion.<sup>50–52</sup> Even if these physical processes may not directly cause significant isotope fractionation (see above) their presence can still bias estimates. Specifically, if water parcels mix in which a different extent of degradation has taken place, isotope values of the mixture will always underestimate the true degradation.<sup>19,50,53</sup> On the other hand, if transformation kicks in after non-degradative processes have already reduced the contaminant concentration, isotope-based estimates can overestimate the true extent of transformation. The reason is that degradation may act on only part of the contaminant load and isotope values would not pick up this fact.<sup>28,51</sup> The importance of these effects has been considered in theoretical treatments.<sup>19,28,53</sup> Useful scenarios and equations have been derived to further constrain these uncertainties with knowledge about the hydrogeology of contaminated sites.<sup>19,28,53</sup>

**Beyond monitoring: what can we learn from observable isotope fractionation?** These examples show that even when isotope measurements are used in a pragmatic approach, a point is quickly reached where it is no longer sufficient to regard the natural system as a black box. Instead, a process understanding is required to reduce uncertainties and to understand the mechanisms of natural attenuation as a basis to predict the effectiveness of natural attenuation in the long run. Can observable isotope fractionation elucidate by what transformation mechanisms or degradation pathways contaminants are broken down? Are aerobic or anaerobic processes at work? Can this information be used to constrain the values of  $\alpha$  and  $\varepsilon$  for quantification of biodegradation? Is it even possible to distinguish biotic from abiotic degradation? This critical review aims to answer these questions by discussing the different factors which together create observable isotope fractionation: (1) the transition state of the underlying (bio)chemical transformation, (2) the way how position-specific isotope effects are reflected in the compound average measured by GC-IRMS, (3) the rate-determining step(s) of natural multistep processes, (4) the product yield in the case of simultaneously occurring, competing degradation pathways. Prospects and limitations for the elucidation of natural transformation mechanisms are discussed, and an outlook is given on ongoing developments.



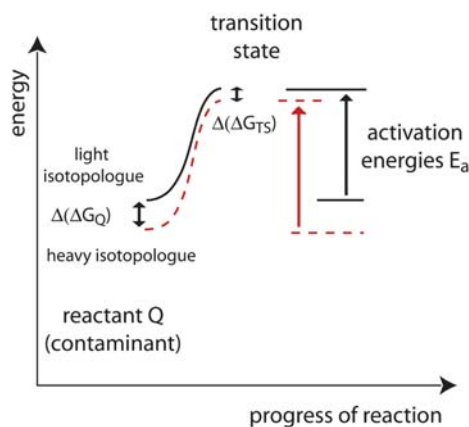


**Fig. 1** Energy differences between isotopologues (molecules containing light *versus* heavy isotopes) during contaminant transformation. The kinetic isotope effect is caused by the difference in activation energies  $\Delta(E_a)$  which, in turn, depends on the energy differences between isotopologues of the reactant,  $\Delta(\Delta G_Q)$ , and of the transition state,  $\Delta(\Delta G_{TS})$ .

## II. Deriving transformation mechanisms from isotope fractionation

**Position-specific isotope effects: Glimpsing at transition states of (bio)chemical reactions.** Kinetic isotope effects arise when a light isotope in a particular position of an organic compound is substituted by a heavy isotope (e.g.,  $^{12}\text{C}$  by  $^{13}\text{C}$ )

$$^{13}\text{C} - \text{KIE} = \text{KIE}_C = \frac{^{12}k}{^{13}k} \quad (5)$$

$^{13}k$  is the rate constant of the molecule with  $^{13}\text{C}$  in the molecular position (*i.e.*, the heavy isotopologue), and  $^{12}k$  is the rate constant of the light isotopologue. From their chemical properties (nuclear charge, number of electrons) isotopes of the same element would be expected to behave in exactly the same way. If they react with different rates nevertheless, it is because (i) the presence of additional neutrons affects the mass involved in atomic motions causing *mass-dependent fractionation*. In addition, (ii) the magnetic moment or nuclear volume of atomic nuclei may change causing *mass-independent fractionation*. Mass-independent fractionation does not play a major role in biological degradation of organic compounds, however. Magnetic isotope effects,<sup>54</sup> or decomposition of photoexcited states<sup>55</sup> are primarily important in photochemical transformations,<sup>56</sup> whereas the nuclear volume effect is significant only for very heavy elements such as Hg.<sup>57,58</sup>

For mass-dependent fractionation, on the other hand, rate constants  $k$ , and activation energies  $E_a$  can be thought to depend on the energy difference between reactants  $Q$  and transition state  $TS$  according to the Arrhenius equation

$$k = A \cdot \exp\{-(E_a)/RT\} = A \cdot \exp\{-(\Delta G_{TS} - \Delta G_Q)/RT\} \quad (6)$$

so that isotope effects are determined by

$$\begin{aligned} \text{KIE}_C &= \frac{^{12}k}{^{13}k} = \frac{^{12}A}{^{13}A} \cdot \exp\left\{-\frac{[\Delta(E_a)]}{RT}\right\} \\ &= \frac{^{12}A}{^{13}A} \cdot \exp\left\{-\frac{[\Delta(\Delta G_{TS}) - \Delta(\Delta G_Q)]}{RT}\right\} \end{aligned} \quad (7)$$

$A$  is the pre-exponential factor of the Arrhenius equation,  $R$  is the universal gas constant and  $T$  is the absolute temperature.  $\Delta(\Delta G_Q)$  is the difference in Gibbs energies between isotopologues of the reactants,  $\Delta(\Delta G_{TS})$  is the analogous difference between isotopologues in the transition state.  $\Delta(E_a)$  is the resulting difference of activation energies which causes the isotope effect. In the case of hydrogen, isotope effects may become even greater, because lighter isotopes can tunnel preferentially through activation barriers.<sup>59</sup>

As illustrated in Fig. 1, kinetic isotope effects may be understood when looking at energy differences between the isotopologues,  $\Delta(\Delta G)$ . Heavy isotopologues are always slightly more stable than light isotopologues. During transformations, bonds are generally weakened so that the isotopic energy difference in the transition state,  $\Delta(\Delta G_{TS})$ , is smaller than on the side of the reactants  $\Delta(\Delta G_Q)$  (see Fig. 1). Consequently, light isotopes have lower activation energies and normally react faster. Values of  $\text{KIE} > 1$  are therefore called normal isotope effects. Vice versa, isotope effects are termed inverse in the rare case that  $\Delta(\Delta G_{TS}) > \Delta(\Delta G_Q)$  and  $\text{KIE} < 1$  corresponding to stiffer bonds (= vibrations of higher energy) in the transition state. Chemistry and geosciences have created different conventions to express the magnitude and direction of isotope fractionation. To avoid ambiguities it is helpful to speak of *normal isotope fractionation* if heavy isotopes become enriched in the reactant – this is the usual case for kinetic isotope fractionation – and of *inverse fractionation* if heavy isotopes become enriched in the product.

Such energy differences  $\Delta(\Delta G)$ , in turn, are determined by the atomic motion of the isotopes inside the molecular structure, specifically through (i) molecular vibrations, (ii) molecular rotations and (iii) translation of molecules.<sup>12</sup> For example, if a molecular vibration more strongly involves the position where an isotopic substitution has taken place, and if the energy of this molecular vibration is greater (corresponding to stiffer bonds) this leads to a greater difference  $\Delta(\Delta G)$ .<sup>14,60</sup> Because of this strong dependence on molecular geometry, isotope effects are an expedient way of investigating transition states of (bio)chemical reactions; in comparison with computational calculations, they essentially allow taking a glimpse at transition state structures. Numerous (bio)chemical studies have synthesized molecules labelled with isotopes in specific molecular positions,<sup>61</sup> or position-specific NMR measurements were conducted.<sup>62</sup> Subsequent determination of kinetic isotope effects made it possible to elucidate transition states of organic reactions and to unravel the mechanism of enzyme catalysis.<sup>63–65</sup> In such interpretations, variational transition-state theory with multidimensional tunnelling is the state-of-the-art theoretical treatment,<sup>66</sup> rather than the simple Arrhenius model considered here.

**How are position-specific isotope effects reflected in the compound average?** The example of atrazine will be used to illustrate the way how position-specific isotope effects are represented in the compound average measured by GC-IRMS. Atrazine belongs to the worldwide most prominent groundwater contaminants. Current studies evaluate isotope fractionation measurements as a new approach to investigate its fate in the environment.<sup>56,67–69</sup> The chemical hydrolysis of atrazine to hydroxyatrazine at pH 12 was subject of two recent publications, one computing position-specific isotope effects<sup>67</sup> (Fig. 2), and the

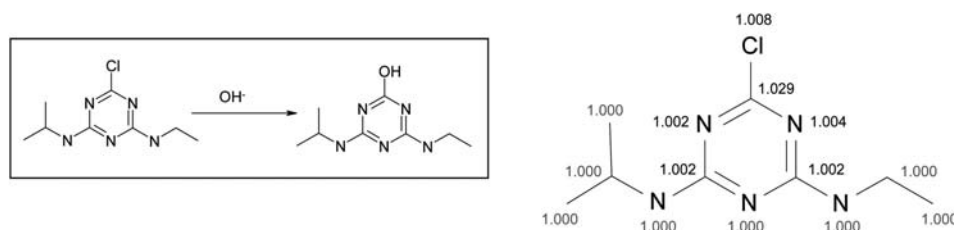


**Fig. 2** Position-specific isotope effects for substitution of  $^{12}\text{C}$  by  $^{13}\text{C}$ , and of  $^{14}\text{N}$  by  $^{15}\text{N}$ , respectively, calculated for the alkaline hydrolysis of atrazine at pH 12.<sup>67</sup>

other reporting experimental data of compound-specific isotope analysis.<sup>68</sup> The underlying mechanism is a nucleophilic aromatic substitution, where a hydroxide ion directly replaces the chlorine substituent.

The computed values for this reaction illustrate that isotopic discrimination occurs primarily in the reacting C–Cl bond. Such strong isotope effects in the reacting bond are called *primary isotope effects*. In comparison, smaller isotopic discrimination is found in adjacent positions. These smaller isotope effects next to the reacting bond are called *secondary isotope effects*. Finally, the example illustrates that isotope discrimination in more distant positions is negligible.

For the interpretation of isotope fractionation measurements by GC-IRMS it is essential to understand how position-specific isotope effects are reflected in the fractionation factor  $\alpha$  determined according to eqn (3). The parameter  $\alpha$  is more accurately termed “kinetic isotope fractionation factor  $\alpha_{\text{P,Q}}^{\text{kin}}(^{13}\text{C}/^{12}\text{C})$  for transformation of compound Q to product P” and is defined as

$$\alpha_{\text{P,Q}}^{\text{kin}}(^{13}\text{C}, ^{12}\text{C}) = \frac{\left(\frac{^{13}\text{C}}{^{12}\text{C}}\right)_{\text{P}}^{\text{instantaneous}}}{\left(\frac{^{13}\text{C}}{^{12}\text{C}}\right)_{\text{Q}}} = \frac{\left(\frac{^{13}\text{C}}{^{12}\text{C}}\right)_{\text{Q}}^{\text{reacting}}}{\left(\frac{^{13}\text{C}}{^{12}\text{C}}\right)_{\text{Q}}} = \frac{d^{13}\text{C}_{\text{Q}}/d^{12}\text{C}_{\text{Q}}}{^{13}\text{C}_{\text{Q}}/^{12}\text{C}_{\text{Q}}} \quad (8)$$

where  $(^{13}\text{C}/^{12}\text{C})_{\text{Q}}$  is the isotope ratio of the reacting contaminant Q, while  $(^{13}\text{C}/^{12}\text{C})_{\text{P}}^{\text{instantaneous}}$  and  $(^{13}\text{C}/^{12}\text{C})_{\text{Q}}^{\text{reacting}}$  are the isotope ratios of momentarily formed product(s) P and disappearing reactant Q, respectively. When integrating this expression, the Rayleigh equation is directly obtained.<sup>23</sup> The corresponding expression in the Delta notation is

$$\begin{aligned} \varepsilon_{\text{P,Q}}^{\text{kin}}(^{13}\text{C}, ^{12}\text{C}) &= \left[ \alpha_{\text{P,Q}}(^{13}\text{C}, ^{12}\text{C}) - 1 \right] \\ &= \left[ \frac{\delta^{13}\text{C}_{\text{P}} + 1}{\delta^{13}\text{C}_{\text{Q}} + 1} - 1 \right] = \frac{\delta^{13}\text{C}_{\text{P}} - \delta^{13}\text{C}_{\text{Q}}}{\delta^{13}\text{C}_{\text{Q}} + 1} \\ &\approx \delta^{13}\text{C}_{\text{P}} - \delta^{13}\text{C}_{\text{Q}} \end{aligned} \quad (9)$$

Two important differences of these expressions to the definition of kinetic isotope effects (eqn (5)) become apparent.

(1) In kinetic isotope effects, light isotopes appear in the numerator, whereas in fractionation factors they appear in the denominator. If light isotopes react faster and isotope fractionation is normal, *KIE* values are therefore greater than one.

$\alpha$  values, in contrast, are smaller than one and  $\varepsilon$  values are negative in the case of normal isotope effects.

(2) Kinetic isotope effects are position specific. In contrast, GC-IRMS measurements convert target compounds into  $\text{CO}_2$ ,  $\text{N}_2$  or  $\text{H}_2$  so that the position specific information gets lost in the compound average.<sup>25</sup> If changes in isotope ratios are small such as typically for C and N, bulk isotope fractionation factors  $\alpha^{\text{kin}}$  calculated from such compound-average data are approximately equal to the average of  $1/\text{KIE}_i$  in all molecular positions  $i$ . For the example of atrazine in Fig. 2 this gives:

$$\alpha_{\text{P,Q}}^{\text{kin}}(^{13}\text{C}, ^{12}\text{C}) \approx \frac{1}{8} \cdot \sum \left( \frac{1}{\text{KIE}_{\text{C},i}} \right) \quad (10)$$

$$\alpha_{\text{P,Q}}^{\text{kin}}(^{15}\text{N}, ^{14}\text{N}) \approx \frac{1}{5} \cdot \sum \left( \frac{1}{\text{KIE}_{\text{N},i}} \right) \quad (11)$$

This calculation implicitly assumes that intramolecular differences in isotope ratios are small throughout the reaction. Otherwise compounds would be labelled, and the  $\text{KIE}_i$  of the labelled position would dominate the observable  $\alpha$ .<sup>25</sup>

Using the computed values of Fig. 2,  $\varepsilon^{\text{kin}}(^{13}\text{C}/^{12}\text{C}) \approx -4\text{‰}$  and  $\varepsilon^{\text{kin}}(^{15}\text{N}/^{14}\text{N}) = -1.2\text{‰}$  are calculated. The calculated average carbon isotope fractionation of  $\varepsilon^{\text{kin}}(^{13}\text{C}/^{12}\text{C}) \approx -4\text{‰}$  is clearly much smaller than the computed position-specific isotope effect of 29 per mill (*i.e.*,  $\text{KIE} = 1.029$ ), but it still indicates the presence of a primary kinetic isotope effect. The calculated  $\varepsilon^{\text{kin}}(^{15}\text{N}/^{14}\text{N}) = -1.2\text{‰}$  of nitrogen, in contrast, illustrates the imprint of secondary isotope effects. While small, they occur in more than one position simultaneously and, therefore, add up to a contribution that would be comparatively small in the presence of a primary isotope effect, but is significant in its absence.<sup>25</sup> Both values agree qualitatively with the experimental results of  $\varepsilon^{\text{kin}}(^{13}\text{C}/^{12}\text{C}) = -5.6\text{‰} \pm 0.1\text{‰}$  and  $\varepsilon^{\text{kin}}(^{15}\text{N}/^{14}\text{N}) = -1.2\text{‰} \pm 0.1\text{‰}$ .<sup>68</sup>

This case illustrates that compound-specific isotope measurements do not provide the same level of insight as position-specific effects. From values of  $\alpha$  or  $\varepsilon$  it is not possible, for example, to tell directly at what molecular position a reaction occurs. Still, the observable fractionation preserves the *nature* of the position-specific effects. Specifically, compound-specific data of the alkaline atrazine hydrolysis tells us that isotope effects are primary for carbon and secondary for nitrogen, and that they are normal rather than inverse. From this it can be concluded that the transformation affects a carbon, but not a nitrogen atom, and that bonds at this carbon centre are weakened. The glimpse at the

transition state is, therefore, to some extent preserved. The next section will discuss how even more detailed mechanistic information may be recovered by a careful evaluation.

**Linking observable isotope fractionation to transformation mechanisms.** In the early 2000s an increasing number of isotopic enrichment factors  $\epsilon^{\text{kin}}$  was published.<sup>24</sup> Questions came up with respect to their variability and representativeness. Particularly intriguing was the case of carbon isotope fractionation measured for aerobic biodegradation of the chlorinated solvent 1,2-dichloroethane (1,2-DCA) in enrichment cultures from a contaminated site. Rather than being constant, or varying randomly,  $\epsilon^{\text{kin}}$  values for carbon showed a binomial distribution, clustering either around  $-4\text{‰}$ , or around  $-29\text{‰}$ .<sup>70,71</sup>

Considering that the two carbon atoms in 1,2-DCA are chemically equivalent, any  $^{13}\text{C}$  isotope in 1,2-DCA has to compete with its twin carbon centre for reaction. Since at natural abundance only one of the two centres is occupied by  $^{13}\text{C}$ , the following equations apply.

$$-\frac{d[^{12}\text{CH}_2\text{Cl}-^{12}\text{CH}_2\text{Cl}]}{dt} = {}^{12}k \cdot [^{12}\text{CH}_2\text{Cl}-^{12}\text{CH}_2\text{Cl}] \quad (12)$$

$$\begin{aligned} -\frac{d[^{13}\text{CH}_2\text{Cl}-^{12}\text{CH}_2\text{Cl}]}{dt} \\ = \left( \frac{{}^{13}k}{2} + \frac{{}^{12}k_{\text{next to }^{13}\text{C}}}{2} \right) \cdot [^{13}\text{CH}_2\text{Cl}-^{12}\text{CH}_2\text{Cl}] \end{aligned} \quad (13)$$

$$\begin{aligned} \alpha_{\text{P,Q}}^{\text{kin}}(^{13}\text{C}, ^{12}\text{C}) &= \frac{d^{13}\text{C}_Q/d^{12}\text{C}_Q}{^{13}\text{C}_Q/^{12}\text{C}_Q} = \frac{\left( \frac{{}^{13}k}{2} + \frac{{}^{12}k_{\text{next to }^{13}\text{C}}}{2} \right)}{{}^{12}k} \\ &= \left( \frac{1}{2} \cdot \frac{{}^{13}k}{{}^{12}k} + \frac{1}{2} \cdot \frac{{}^{12}k_{\text{next to }^{13}\text{C}}}{{}^{12}k} \right) \end{aligned} \quad (14)$$

Neglecting secondary isotope effects (*i.e.*, assuming that  ${}^{12}k_{\text{next to }^{13}\text{C}} = {}^{12}k$ ) this simplifies to

$$\begin{aligned} \epsilon_{\text{P,Q}}^{\text{kin}}(^{13}\text{C}, ^{12}\text{C}) &= \alpha_{\text{P,Q}}^{\text{kin}}(^{13}\text{C}, ^{12}\text{C}) - 1 = \left( \frac{1}{2} \cdot \frac{{}^{13}k}{{}^{12}k} + \frac{1}{2} \right) - 1 \\ &= \frac{1}{2} \cdot \left( \frac{{}^{13}k}{{}^{12}k} - 1 \right) \end{aligned} \quad (15)$$

$$\frac{{}^{12}k}{{}^{13}k} = \frac{1}{2 \cdot \epsilon_{\text{P,Q}}^{\text{kin}}(^{13}\text{C}, ^{12}\text{C}) + 1} \quad (16)$$

Plugging in the values of  $-4\text{‰}$  and  $-29\text{‰}$ , kinetic isotope effects were estimated as 1.01 and 1.06.<sup>72</sup> The first value is consistent with a C–H bond oxidation, whereas the second is highly indicative of a second-order nucleophilic substitution ( $\text{S}_{\text{N}}2$  reaction) – hardly any other type of reaction is associated with such large carbon kinetic isotope effects.<sup>14,25</sup> The analysis was confirmed by carbon isotope fractionation measurements with pure strains of known transformation mechanisms,<sup>72</sup> and was subsequently used to probe for the mechanism under nitrate-

reducing conditions.<sup>73</sup> Through a careful analysis in terms of position-specific isotope effects, the binomial distribution of enrichment factors could therefore be linked to different underlying transformation mechanisms!

Almost simultaneously, the same approach made it possible to infer for the first time the transformation mechanism of anaerobic methyl *tert*-butyl ether (MTBE) degradation. After replacing tetraethyl lead in gasoline, MTBE has become an important groundwater contaminant, and its natural attenuation has been of great interest.<sup>8</sup> Carbon  $\epsilon^{\text{kin}}$  values of MTBE measured with microbial cultures clustered around  $-2\text{‰}$  for aerobic degradation,<sup>74,75</sup> but around  $-9\text{‰}$  for anaerobic degradation;<sup>29</sup> hydrogen  $\epsilon^{\text{kin}}$  values showed the opposite trend, clustering around  $-40\text{‰}$  in aerobic degradation<sup>74</sup> and around only  $-10\text{‰}$  in anaerobic degradation.<sup>29</sup> A careful analysis in terms of kinetic isotope effects showed that the pronounced hydrogen and small carbon isotope fractionation under aerobic conditions was again consistent with C–H bond cleavage.<sup>25,30</sup> In contrast, the large carbon isotope fractionation and small, secondary hydrogen isotope effects could pinpoint for the first time an  $\text{S}_{\text{N}}2$  reaction as only possible mechanism under anaerobic conditions.<sup>25,30</sup>

Another important impulse of this work was the visualization of the different contaminant degradation pathways in dual (“two-dimensional”) isotope plots<sup>25,29,30</sup> adapting a practice well established in geochemistry<sup>76–78</sup> (see Fig. 3). The observable slope was shown to be approximately equal to the ratio of enrichment factors

$$\frac{\Delta\delta^2\text{H}}{\Delta\delta^{13}\text{C}} \approx \frac{\epsilon_{\text{H}}}{\epsilon_{\text{C}}} \quad (17)$$

and was even linked to underlying kinetic isotope effects (see eqn (23) below).<sup>15,25</sup> Numerous studies have followed this approach leading to a substantial body of mechanistic dual isotope investigations on various contaminant classes involving benzene,<sup>79,80</sup> toluene,<sup>81–83</sup> nitrobenzene,<sup>84</sup> RDX,<sup>85</sup> atrazine,<sup>68,69,86</sup> isoproturon<sup>87,88</sup> and chlorinated ethylenes.<sup>89,90</sup> Table 1 provides a summary of mechanistic environmental isotope fractionation studies reported in recent years. For the case of MTBE, follow-up studies have found some variability in isotope fractionation under aerobic conditions,<sup>91–93</sup> by alternative mechanisms<sup>15</sup> and associated with volatilization.<sup>21</sup> Although the range of possible dual isotope plots for MTBE has therefore broadened, the picture of Fig. 3 remains valid that small hydrogen and large carbon isotope fractionation are strongly indicative of anaerobic MTBE degradation.

**Prospects and limitations of mechanistic elucidations from compound-specific isotope studies.** These examples illustrate important aspects about isotope fractionation in transformation reactions of organic contaminants.

**(1) Isotope fractionation gives insight that would not be obtained from product analysis.** Specifically, aerobic and anaerobic MTBE transformation, as well as acid hydrolysis,<sup>15</sup> generate *tert*-butyl alcohol as common transformation product, which would indicate at first sight a common transformation pathway. Isotope fractionation, in contrast, can delineate differences in the transformation mechanisms, because it reflects the different transition

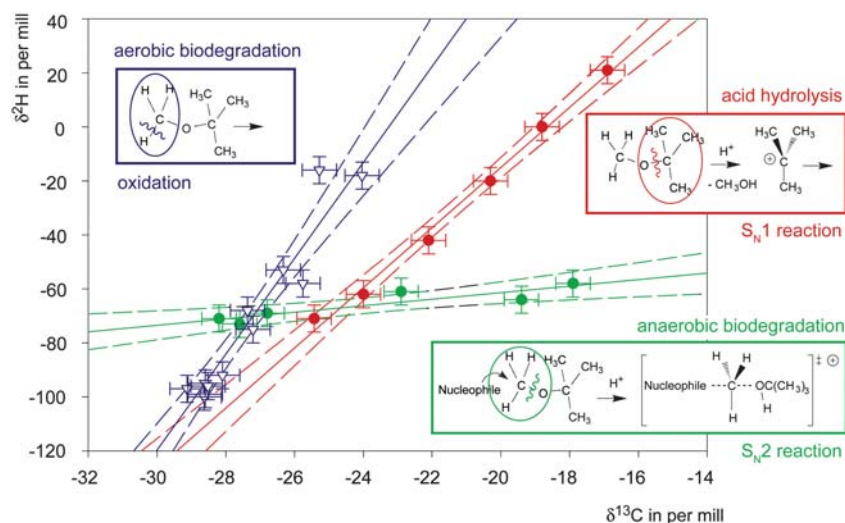


**Fig. 3** Changes in carbon and hydrogen isotope ratios of methyl *tert*-butyl ether (MTBE) observed during different transformation reactions: aerobic biodegradation (inverted triangles), anaerobic biodegradation (circles) and acid hydrolysis (circles); adapted from ref. 15 Error bars indicate the total uncertainty of  $\pm 0.5\text{‰}$  for carbon and  $\pm 5\text{‰}$  for hydrogen,<sup>3,10</sup> while dashed lines give 95% confidence intervals of the linear regressions. For each transformation, the respective mechanism is indicated by a circle around the reactive position and a sinuous line across the broken bond.

states. Information is, therefore, given about the strategy of microorganisms to break down contaminants at the enzymatic level.

**(2) Evidence from isotope fractionation may elucidate degradation pathways even if no products are detected** such as with 1,2-DCA. The reason is that the transformation leaves its imprint in the reacting contaminant in the form of characteristic changes in isotope ratios. Transformation mechanisms and associated degradation pathways can therefore be inferred from isotope analysis of the parent compound alone, even without detection of metabolites!

**(3) Isotope fractionation is mechanism-specific.** Isotope fractionation bears potential to distinguish aerobic *versus* anaerobic degradation if (a) the degradation involves different transformation mechanisms such in the case of MTBE, and if (b) these mechanisms are reflected in different dual isotope plots. Occasionally, however, similar mechanisms prevail under different redox conditions,<sup>82</sup> or different pathways may produce similar dual isotope plots.<sup>85</sup> Besides, more than one mechanism can occur aerobically, such as observed with 1,2-DCA. Therefore, isotope fractionation is first and foremost mechanism-specific. *A coincidence with pathways, products, redox conditions or the abiotic/biotic nature of transformation is, strictly speaking, coincidental.* Nonetheless such information may often be obtained, particularly if different elements are involved in different bonds such as in aerobic *versus* anaerobic degradation of nitroaromatic compounds.<sup>84</sup> Very recently, first examples have been reported where observable isotope fractionation could even reflect the abiotic *versus* biotic character of a transformation.<sup>39,88,94</sup> Table 1 gives a summary of existing mechanistic isotope fractionation studies of organic groundwater contaminants. Information is provided about investigated compounds, the prospect of resolving competing pathways, and potential improvements to provide further mechanistic insight. These aspects will be discussed in more detail in the concluding section.

**(4) Compound-specific isotope fractionation must be evaluated in mechanistic scenarios.** As discussed above, compound-specific measurements can not directly indicate at what molecular position a reaction occurs. When evaluating isotope fractionation to resolve the transformation mechanism from kinetic isotope effects, the following stepwise approach must therefore be taken.<sup>25</sup> (A) All transformation mechanisms must be considered that may possibly occur – it is the goal to confirm or discard them. (B) For each mechanism and each element, the total number of atoms ( $n$ ) must be determined, as well as the number of atoms ( $x$ ) that would experience isotope effects in the given mechanistic scenario (= atoms in reactive positions). Subsequently, it must be considered whether these atoms experience the isotope effect together – such as in concerted reactions or in the case of secondary isotope effects – or whether intramolecular competition occurs, such as in the example of 1,2-DCA above (*i.e.*, only one of several atoms reacts). (C) Finally, kinetic isotope effects can be estimated, and their magnitude may be compared with typical isotope effects for the given mechanistic scenario. If the magnitude is consistent, the mechanistic scenario must be considered possible, if not, it can be discarded.

*How to estimate position-specific isotope effects from “bulk” fractionation data of the compound average.* This evaluation essentially calculates how large position-specific isotope effects would be if the total observable isotope fractionation was only attributed to the reactive positions identified in step B. Such an evaluation may be accomplished according to the following procedure brought forward by Elsner *et al.*<sup>25</sup>

(I) Determine the changes in isotope ratios that occur specifically in the reacting position(s). This is done by multiplying the changes in isotope ratios of the compound-average by the factor  $n/x$  (see above). In this context, intramolecular isotope ratio differences are assumed to be small, as recently confirmed experimentally for hydrogen in MTBE.<sup>95</sup>

(II) Apply the Rayleigh equation to these corrected isotope ratios to evaluate the isotopic enrichment factor in the reactive



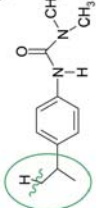
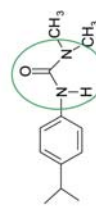
**Table 1** Summary of mechanistic isotope fractionation studies of organic groundwater contaminants

Compound	Competing Mechanisms	Distinction possible?	Distinction based on	Ref.	Further evidence expected from
1,2-Dichloroethane	 C-H bond oxidation S <sub>N</sub> -2-reaction	Yes	Evaluation in terms of <i>AKIE</i> values	Hunkeler <i>et al.</i> 2000 <sup>70</sup> Hirschorn <i>et al.</i> 2004 <sup>72</sup> Elsner <i>et al.</i> 2005 <sup>25</sup> Hirschorn <i>et al.</i> 2007 <sup>73</sup> Abe <i>et al.</i> 2009 <sup>97</sup>	Chlorine and hydrogen isotope analysis
MTBE	 C-H bond oxidation + volatilization S <sub>N</sub> -2-reaction S <sub>N</sub> -1-reaction	Yes	Dual (C, H) Isotope Slopes, Evaluation in terms of <i>AKIE</i> values	Hunkeler <i>et al.</i> 2001 <sup>75</sup> Gray <i>et al.</i> 2002 <sup>74</sup> Zwank <i>et al.</i> 2005 <sup>30</sup> Kuder <i>et al.</i> 2005 <sup>29</sup> Elsner <i>et al.</i> 2005 <sup>25</sup> Rosell <i>et al.</i> 2007 <sup>91</sup> Elsner <i>et al.</i> 2007 <sup>15</sup> McKelvie <i>et al.</i> 2009 <sup>134</sup> Kuder <i>et al.</i> 2009 <sup>21</sup>	Oxygen isotope analysis, Position-specific isotope analysis
Benzene	 Anaerobic biodegradation, different terminal electron acceptors Aerobic biodegradation, ring monooxygenase Aerobic biodegradation, ring dioxygenase	Anaerobic <i>versus</i> aerobic: Yes Different terminal electron acceptors: Possibly	Dual (C, H) Isotope Slopes	Hunkeler <i>et al.</i> 2001 <sup>162</sup> Mancini <i>et al.</i> 2003 <sup>163</sup> Fischer <i>et al.</i> 2008 <sup>79</sup> Mancini <i>et al.</i> 2008 <sup>80</sup>	Further dual isotope studies to corroborate trends observed to date
Toluene	 Anaerobic biodegradation, benzyl succinate synthase Aerobic biodegradation, methyl monooxygenase Aerobic biodegradation, ring monooxygenase Aerobic biodegradation, ring dioxygenase	Ring oxidation <i>versus</i> methyl group oxidation: Yes Different terminal electron acceptors: Possibly	Dual (C, H) Isotope Slopes	Ward <i>et al.</i> 2000 <sup>164</sup> Morasch <i>et al.</i> 2001 <sup>165</sup> Morasch <i>et al.</i> 2002 <sup>166</sup> Morasch <i>et al.</i> 2004 <sup>88</sup> Mancini <i>et al.</i> 2006 <sup>81</sup> Tobler <i>et al.</i> 2007 <sup>167</sup> Tobler <i>et al.</i> 2008 <sup>83</sup> Vogt <i>et al.</i> 2008 <sup>82</sup>	
Polychlorinated ethanes	 C-Cl bond reduction (only geminal C-Cl) C-Cl bond reduction (vicinal C-Cl) Dehydrochlorination	Possibly	Carbon <i>AKIE</i> values, intramolecular bulk chlorine isotope effects	Elsner <i>et al.</i> 2007 <sup>145</sup> Hofstetter <i>et al.</i> 2007 <sup>154</sup> VanStone <i>et al.</i> 2008 <sup>146</sup>	Compound-specific chlorine and hydrogen isotope analysis

Table 1 (Contd.)

Compound	Competing Mechanisms	Distinction possible?	Distinction based on	Ref.	Further evidence expected from
Nitrobenzene	<p>versus</p> <p>Aerobic biodegradation, ring dioxygenase</p> <p>Anaerobic biodegradation, nitro group reduction</p>	Yes	Dual (C, N) Isotope Slopes	Hofstetter <i>et al.</i> 2008 <sup>84</sup>	
RDX	<p>Aerobic denitration</p> <p>Anaerobic nitro group reduction</p>	(Yes) (very similar dual isotope slopes)	Dual (N, O) Isotope Slopes	Bernstein <i>et al.</i> 2008 <sup>85</sup>	Compound-specific carbon, nitrogen and hydrogen isotope analysis
Chlorinated ethylenes	<p>Abiotic Transformation by Zero Valent Iron</p> <p>Dichloroelimination</p> <p>Hydrogenolysis</p> <p>Biodegradation</p>	Yes	Characteristic carbon isotope value evolution in reaction products	Elsner <i>et al.</i> 2008 <sup>84</sup>	Compound specific chlorine and hydrogen isotope analysis
<i>cis</i> -Dichloroethylene, vinyl chloride	<p>Aerobic degradation (epoxidation)</p> <p>Anaerobic degradation (reductive dehalogenation)</p> <p>Nucleophile</p>	Yes	Dual (C, Cl) Isotope Slopes	Abe <i>et al.</i> 2009 <sup>89</sup>	
Atrazine	<p>Alkaline Hydrolysis</p> <p>Acidic Hydrolysis / Biotransformation to Hydroxyatrazine</p> <p>Dealkylation via C-H bond oxidation</p>	Biotic hydrolysis versus dealkylation: Yes Acidic <i>versus</i> alkaline hydrolysis: Yes	Dual (C, N) Isotope Slopes (+H isotope analysis)	Meyer <i>et al.</i> 2008 <sup>88</sup> Hartenbach <i>et al.</i> 2008 <sup>86</sup> Meyer <i>et al.</i> 2009 <sup>89</sup>	Compound specific hydrogen isotope analysis

Table 1 (Contd.)

Compound	Competing Mechanisms	Distinction possible?	Distinction based on	Ref.	Further evidence expected from
Isoproturon	<p>   fungal hydroxylation </p> <p>   abiotic hydrolysis versus bacterial hydrolysis </p>	Yes	Triple (C, N, H) Isotope Slopes, position-specific isotope analysis	Penning <i>et al.</i> 2008 <sup>87</sup> Penning <i>et al.</i> 2010 <sup>88</sup>	

position,  $\epsilon_{\text{reacting position}}$ . For all elements except for hydrogen, this value may alternatively be obtained in good approximation as

$$\epsilon_{\text{reacting position}} \approx \frac{n}{x} \cdot \epsilon_{\text{compound average}} \quad (18)$$

When applied to hydrogen data, in contrast, eqn (18) can lead to unrealistically high values;<sup>25,15</sup> for this element, therefore, the exact procedure should be followed (*i.e.*, (I) multiply isotope changes by  $n/x$  to determine  $\delta^2\text{H}$  in the reacting position, (II) apply the Rayleigh equation to this modified  $\delta^2\text{H}$  data).

(III) Calculate the apparent (= observable) kinetic isotope effect (*AKIE*) at the reacting position in the absence of intramolecular competition according to

$$AKIE = \frac{1}{\epsilon_{\text{reacting position}} + 1} \quad (19)$$

and in the presence of intramolecular competition according to

$$AKIE = \frac{1}{z \cdot \epsilon_{\text{reacting position}} + 1} \quad (20)$$

where  $z$  is the number of atoms that are in intramolecular competition. Like in the example of 1,2-DCA it is assumed again that primary isotope effects dominate secondary ones so that the latter are neglected. Although recent studies<sup>15,67</sup> point out the uncertainty associated with this approach, the example of the computed atrazine isotope values above actually suggests that the error introduced by this assumption is small.

**(5) Observable isotope fractionation becomes smaller for larger molecules.** For the typical case of  $x = z$  (meaning that all chemically equivalent atoms in a reactive position compete for reaction) the following approximate equation applies

$$AKIE = \frac{1}{z \cdot \epsilon_{\text{reacting position}} + 1} \approx \frac{1}{z \cdot \frac{n}{x} \cdot \epsilon_{\text{compound average}} + 1} \approx \frac{1}{n \cdot \epsilon_{\text{compound average}} + 1} \cdot \epsilon_{\text{compound average}} = \frac{1}{n} \left( \frac{1}{AKIE} - 1 \right) \quad (21)$$

In other words, observable isotope fractionation becomes smaller if more atoms of the same element are present within a compound. This reflects the fact that the actual isotope effect occurs in the reacting bond and that additional atoms tend to “dilute” this fractionation in the compound average, as illustrated for the case of atrazine above. Further examples are the reductive transformation of nitroaromatic compounds, where multiple nitro substituents reduce observable nitrogen isotope fractionation,<sup>96</sup> or the dehalogenation of chloroalkanes, where observable carbon isotope fractionation becomes smaller with increasing number of carbon atoms.<sup>97</sup> As repeatedly pointed out,<sup>24,25,98</sup> an upper limit therefore exists for the size of compounds that can realistically be investigated by compound-specific isotope fractionation. For example, if the position-specific fractionation is assumed as 30‰ (*i.e.*,  $AKIE = 1.03$ ) and if the minimum acceptable fractionation in the compound-average is 2‰ (*i.e.*,  $\epsilon^{\text{kin}} = -2\text{‰}$ ), the maximum number of atoms that may be present of this element would be 15. This number can become larger or smaller depending on the magnitude of the position-specific isotope effect. Interestingly, secondary isotope

effects are less affected by the effect of dilution because they occur in several positions simultaneously so that – in the absence of primary isotope effects – the fractionation in the compound average is given as

$$\varepsilon_{\text{compound average}} = \frac{x}{n} \left( \frac{1}{AKIE_{\text{secondary}}} - 1 \right) \quad (22)$$

A telling example is the hydrogen isotope fractionation of MTBE when reacting according to an  $S_N1$  mechanism as shown in Fig. 3. Although no C–H bond is broken, the combined secondary isotope effects of nine hydrogen atoms in the reactive *tert*-butyl group add up to an observable isotope fractionation that is almost as pronounced as the result of a primary isotope effect!<sup>15</sup> Quite generally, the dual isotope plot of contaminant transformations is approximately given as<sup>15,25</sup>

$$\frac{\Delta\delta^2\text{H}}{\Delta\delta^{13}\text{C}} \approx \frac{\varepsilon_{\text{H}}}{\varepsilon_{\text{C}}} \approx \frac{(x/n)_{\text{H}} \cdot \varepsilon_{\text{reactive position,H}}}{(x/n)_{\text{C}} \cdot \varepsilon_{\text{reactive position,C}}} \approx \frac{(x/n)_{\text{H}} \cdot KIE_{\text{H}} - 1}{(x/n)_{\text{C}} \cdot KIE_{\text{C}} - 1} \cdot \frac{1 + KIE_{\text{C}} \cdot (z_{\text{C}} - 1)}{1 + KIE_{\text{H}} \cdot (z_{\text{H}} - 1)} \quad (23)$$

These examples show that a careful evaluation in mechanistic scenarios is important for the correct mechanistic interpretation of observable isotope fractionation data. When properly applied, on the other hand, mechanistic information may be recovered.

**(6) The need for kinetic isotope effect-reference data.** Isotope effect studies face the general difficulty (i) that the evaluation of isotope fractionation requires a mechanistic hypothesis against which experimental data can be compared, and (ii) that accurate isotope effect reference data must be available to verify this mechanistic hypothesis. The first requirement can be challenging in cases where the nature of the initial activation step is truly unknown (e.g., in anaerobic benzene degradation<sup>79,80</sup>). The second requirement emphasizes the need for accurate reference values.

In a pragmatic approach, kinetic isotope effects estimated for a given mechanistic scenario (see above) may be simply compared to typical isotope values reported for the given mechanism.<sup>14,25</sup> This approach works if completely different bonds with different elements are involved<sup>84</sup> or if the transformations involve mechanisms with substantially different isotope fractionation (e.g.,  $S_N2$  reaction *versus* oxidation, like in the examples of 1,2-dichloroethane and MTBE). On the one hand, such data is not always available, however. On the other hand, it is well understood<sup>12,64,65</sup> that – due to the dependence on transition state structures – isotope effects show moderate variations even for the same mechanism. For an environmental transformation this was recently observed in the nucleophilic substitution of chloroalkanes by *Xanthobacter autotrophicus* GJ10.<sup>97</sup>

This emphasizes the need for accurate computational reference data, as has been stressed in particular for mechanistic interpretations of ester aminolysis.<sup>99</sup> Ideally, compound specific isotope investigations would therefore always be accompanied by computational studies such as in the example of atrazine above,<sup>67,68</sup> or like in recent studies on isoproturon hydrolysis<sup>87</sup> or nitroaromatic compound reduction.<sup>86,96</sup> These cases are rare, however. On the one hand, mechanistic compound-specific isotope studies have not yet come to the attention of many computational chemists; on the other hand, environmental transformations are often very challenging to compute, since they typically take place in aqueous solution, may involve poorly defined environmental surfaces and can entail multiple reaction paths (e.g., for proton transfer).

Therefore, if no reference data is available, another pragmatic approach is the interpretation of environmental transformations in comparison with abiotic reference reactions such as in the case of MTBE.<sup>15</sup> A most recent example is the biotransformation of atrazine to hydroxyatrazine where abiotic reference experiments have made it possible to infer the nature of the underlying

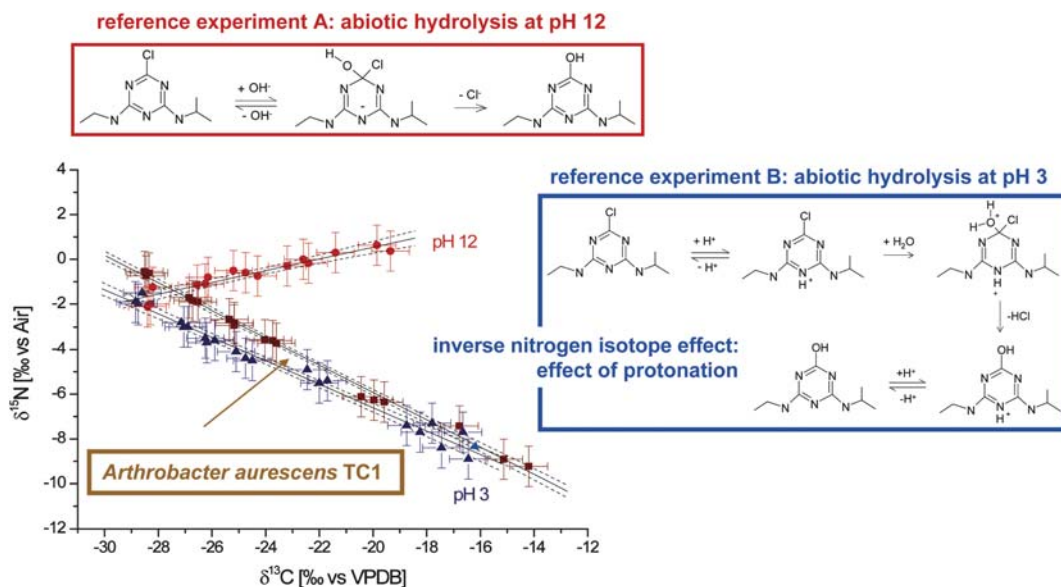


**Fig. 4** Changes in carbon and nitrogen isotope ratios of atrazine during transformation to hydroxyatrazine by *Arthrobacter aureus* TC1, as well as in abiotic reference experiments at pH 3 and pH 12 (adapted from ref. 69). Error bars indicate the total uncertainty of  $\pm 0.5\text{‰}$  for carbon and  $\pm 1\text{‰}$  for nitrogen,<sup>3,10</sup> while dashed lines give 95% confidence intervals of the linear regressions.



enzymatic mechanism.<sup>69</sup> While hydrolysis in aqueous solution at pH 12 showed normal carbon and nitrogen isotope fractionation (see Fig. 2 and 4), isotope fractionation was normal for carbon, but *inverse* for nitrogen when experiments were conducted at pH 3, as well as in biotransformation experiments (Fig. 4).

This observation can be explained by the protonation of a nitrogen atom prior to the nucleophilic aromatic substitution (see scheme in Fig. 4) which creates more constrained bonds around the nitrogen centre with higher vibrational energies in the transition state. Fig. 4 shows the resulting dual isotope slopes together with those of bacterial degradation experiments with *Arthrobacter aurescens* TC1. The agreement of the data at pH 3 with the data for the bacterial hydrolysis demonstrates that the reaction at the enzymatic site must involve a similar strategy of activation by protonation. What is more, microorganisms containing the TrzN enzyme (*Arthrobacter aurescens* TC1) and containing the AtzA enzyme (*Chelatobacter heintzii*) showed an identical trend despite the fact that the amino acid-relatedness between the two enzymes is only 27%. This indicates that the two enzymes must have evolved independently towards catalyzing essentially the same transformation mechanism! This example shows again that isotope fractionation studies at natural abundance can give unique insight into the strategy of microorganisms to break down contaminants at the enzymatic level.

### III. Isotope fractionation in natural multistep reactions

Until now, the focus of this review has been on the mechanism of elementary (bio)chemical reactions. Environmental transformations, however, generally consist of many more steps, as sketched in Fig. 5. A contaminant dissolves from a pure phase NAPL (non aqueous phase liquid). Molecules are subject to advective-dispersive transport and diffuse to the surface of microorganisms or reactive minerals. They may need to pass a cell wall. At surfaces or enzymes they compete with other molecules for a limited number of reaction sites so that the overall kinetics shifts from first- to zero-order. The enzyme reaction itself involves several steps such as co-substrate binding, activation, bond conversion, product release, *etc.* Finally, even purely chemical conversions may entail more than one step like the acidic hydrolysis of atrazine discussed above.

The question arises how these steps are reflected in the observable isotope fractionation. How many steps must be

considered? In what way are they represented? Which is the most important one? How does this affect interpretations?

To answer these questions, isotope fractionation in multistep processes will first be treated conceptually in a steady-state treatment. For environmental reactions such a steady-state treatment is generally appropriate – even if reactant and product concentrations change over time – as long as one or more bottlenecks determine the overall transformation rate. Standing stocks of intermediate build up under such circumstances (*e.g.*, enzyme-substrate complexes, metabolites, *etc.*) the concentration of which does not change over short time intervals. Attention will be given to this mathematical treatment, because it draws the “big picture” of how different processes affect observable isotope fractionation. Subsequently, several examples of natural multistep processes will be discussed to fill the scheme with life. Because the processes of Fig. 5 may have an enormous impact on the isotope fractionation that we observe, also this discussion will be rather detailed, involving examples from the “classical” literature, as well as recent studies on contaminant transformation.

#### Conceptual treatment of isotope effects in multistep reactions.

Isotope fractionation in multistep processes at steady-state is an example where the same conceptual understanding has been derived more or less independently in different disciplines.<sup>100–106</sup> Derivations often look complicated and follow their own nomenclature so that the common underlying principle is not easily discerned. This review will therefore present an own derivation which aims to convey the general idea in an approachable way. Subsequently, it is shown how this treatment accommodates the different expressions derived to date. A brief discussion of enzyme analysis, sulfate reduction and photosynthesis will then show analogies and common principles. After this multistep transformation processes of organic contaminants will be discussed.

**General considerations.** To start with, the isotope effect of a given step *i* can only be observed in the reactant Q if molecules return from step *i* back to Q in order to “report” what has been happening. Consequently, isotope fractionation in multistep processes under steady-state reflects all steps leading up to and incorporating the first irreversible step.

Further, the equilibrium isotope effect of a given step *i* may be defined as (*e.g.*, for carbon)

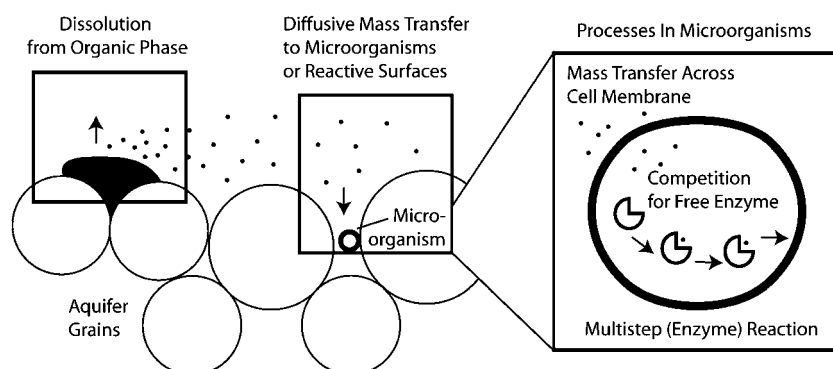


Fig. 5 Examples of possible process steps that may be involved in natural organic contaminant degradation.

$$(EIE_C)_i = \frac{{}^{12}K_i}{{}^{13}K_i} = \frac{({}^{12}k_i/{}^{12}k_{-i})}{({}^{13}k_i/{}^{13}k_{-i})} = \frac{({}^{12}k_i/{}^{13}k_i)}{({}^{12}k_{-i}/{}^{13}k_{-i})} = \frac{(KIE_C)_i}{(KIE_C)_{-i}} \quad (24)$$

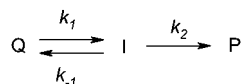
where  $k_i$  and  $k_{-i}$  are rate constants of forward and backward reaction of step  $i$ ,  $K_i$  are the equilibrium constants for light *versus* heavy isotopologues.

Analogous expressions for fractionation factors  $\alpha_i$  and enrichment factors  $\varepsilon_i$  are.

$$\alpha_i^{equ} = \alpha_i^{kin}/\alpha_{-i}^{kin} \quad (25)$$

$$\begin{aligned} \varepsilon_i^{equ} &= \alpha_i^{equ} - 1 = \alpha_i^{kin}/\alpha_{-i}^{kin} - 1 = (\alpha_i^{kin} - \alpha_{-i}^{kin})/\alpha_{-i}^{kin} \\ &= (\varepsilon_i^{kin} - \varepsilon_{-i}^{kin})/\alpha_{-i}^{kin} \approx \varepsilon_i^{kin} - \varepsilon_{-i}^{kin} \end{aligned} \quad (26)$$

**Expressions for a two-step steady state process.** As derived in Table 2 and 3 (or, *e.g.*, ref. 87, 107), for a two-step process:



a steady-state treatment gives the apparent (= observable) kinetic isotope effect as

$$\begin{aligned} AKIE &= \frac{(EIE_1 KIE_2) + \frac{k_2}{k_{-1}} \cdot KIE_1}{1 + \frac{k_2}{k_{-1}}} \\ &= \frac{k_{-1}}{k_{-1} + k_2} \cdot (EIE_1 KIE_2) + \frac{k_2}{k_{-1} + k_2} \cdot KIE_1 \end{aligned} \quad (27)$$

Table 3 shows that the same expression is obtained for Michaelis–Menten catalysis. Therefore, of the molecules that are converted to intermediate I, a fraction  $k_{-1}/(k_{-1} + k_2)$  reacts back to reactant Q, whereas a fraction  $k_2/(k_{-1} + k_2)$  passes on to product P. For molecules of the fraction  $k_2/(k_{-1} + k_2)$  step 1 is already irreversible. Their contribution to the isotope effect in Q is therefore simply given by  $KIE_1$ , in much the same way as in a one-step reaction. Molecules of the fraction  $k_{-1}/(k_{-1} + k_2)$ , in contrast, react back to reactant Q. They can therefore make the imprint of  $KIE_2$ , which acts on all molecules of I, visible in Q. In addition, they are subject to the equilibrium isotope effect

**Table 2** Possible elementary process steps in multistep processes, their rate expressions, and expressions for kinetic isotope effects

Process acting on Q	Chemical equation	Rate equation	Meaning of apparent rate constant	Differential equation for isotopologues of Q	Associated intrinsic kinetic isotope effect for elements in Q
Monomolecular reaction	$Q \xrightarrow{k_1} P$	$-\frac{d[Q]}{dt} = k_1 \cdot [Q]$	$k_{app} = k_1$	$\frac{d[{}^lQ]}{d[{}^hQ]} = \frac{{}^l k_1}{{}^h k_1} \cdot \frac{[{}^lQ]}{[{}^hQ]}$	$KIE_1 = \frac{{}^l k_1}{{}^h k_1}$
Mass transfer <sup>a</sup>	$Q_{\text{location A}} \xrightarrow{k_1} Q_{\text{location B}}$	$F_{net} = k_{ex} \cdot \frac{V}{A} \cdot [Q_B - Q_A]$	$k_{ex} = D \cdot \frac{A}{\delta \cdot V}$	$\frac{d[{}^lQ]}{d[{}^hQ]} = \frac{{}^l k_{ex}}{{}^h k_{ex}} \cdot \frac{[{}^lQ_B - {}^lQ_A]}{[{}^hQ_B - {}^hQ_A]}$	$KIE_1 = \frac{{}^l k_{ex}}{{}^h k_{ex}}$
Bimolecular reaction (two reactants)	$Q + S \xrightarrow{k_1} P$	$-\frac{d[Q]}{dt} = k_1 \cdot [Q] \cdot [S]$	$k_{app} = k_1 \cdot [S]$	$\frac{d[{}^lQ]}{d[{}^hQ]} = \frac{{}^l k_1}{{}^h k_1} \cdot \frac{[{}^lQ] \cdot [S]}{[{}^hQ] \cdot [S]}$ $= \frac{{}^l k_1}{{}^h k_1} \cdot \frac{[{}^lQ]}{[{}^hQ]}$	$KIE_1 = \frac{{}^l k_1}{{}^h k_1}$
Bimolecular reaction (one reactant) <sup>b</sup>	$Q + Q \xrightarrow{k_1} P$	$-\frac{d[Q]}{dt} = k_1 \cdot [Q] \cdot [Q]$	$k_{app} = k_1$ (second order rate constant)	$\frac{d[{}^lQ]}{d[{}^hQ]} = \frac{{}^l k_1}{{}^h k_1} \cdot \frac{[{}^lQ] \cdot [{}^lQ]}{[{}^hQ] \cdot [{}^hQ]}$ $= \frac{{}^l k_1}{{}^h k_1} \cdot \frac{[{}^lQ]}{[{}^hQ]}$	$KIE_1 = \frac{{}^l k_1}{{}^h k_1}$
First step of catalysis ( $C_{free}$ = free catalyst, free enzyme...)	$Q + C_{free} \xrightarrow{k_1} P$	$-\frac{d[Q]}{dt} = k_1 \cdot [Q] \cdot [C_{free}]$	$k_{app} = k_1 [C_{free}]$	$\frac{d[{}^lQ]}{d[{}^hQ]} = \frac{{}^l k_1}{{}^h k_1} \cdot \frac{[{}^lQ] \cdot [C_{free}]}{[{}^hQ] \cdot [C_{free}]}$ $= \frac{{}^l k_1}{{}^h k_1} \cdot \frac{[{}^lQ]}{[{}^hQ]}$	$KIE_1 = \frac{{}^l k_1}{{}^h k_1}$

<sup>a</sup>  $F_{net}$ : net flux;  $V$ : volume of compartment considered;  $A$ : area of interface;  $D$ : diffusivity of compound;  $\delta$ : thickness of interlayer. <sup>b</sup> Expression for heavy isotopes at low abundance taking into account the low probability that two heavy isotopologues come together for reaction.

**Table 3** Possible composite process steps in multistep processes, their rate expressions, and expressions for kinetic isotope effects

Process acting on Q	Chemical equation	Rate equation	Meaning of apparent rate constant $k_{app}$	Differential equation for isotopologues of Q	Associated apparent kinetic isotope effect in Q
Two step process at steady state (first step reversible, second step irreversible)	$\text{Q} \xrightleftharpoons[k_{-1}]{k_1} \text{I} \xrightarrow{k_2} \text{P}$	$-\frac{d[\text{Q}]}{dt} = \frac{d[\text{I}]}{dt} = k_2 \cdot [\text{I}]$ $= \frac{k_1 \cdot k_2}{k_{-1} + k_2} \cdot [\text{Q}]$	$k_{app} = \frac{k_1 \cdot k_2}{k_{-1} + k_2}$	$\frac{d[\text{Q}]}{d[\text{Q}]}$ $= \frac{{}^l k_1 \cdot {}^l k_2}{{}^h k_1 \cdot {}^h k_2} \cdot \frac{{}^h k_{-1} + {}^h k_2}{{}^l k_{-1} + {}^l k_2} \cdot \frac{[\text{Q}]}{[\text{Q}]}$	$AKIE = \frac{{}^l k_1 \cdot {}^l k_2}{{}^h k_1 \cdot {}^h k_2} \cdot \frac{{}^h k_{-1} + {}^h k_2}{{}^l k_{-1} + {}^l k_2}$ $= \frac{EIE_1 \cdot EIE_2 + EIE_1 \cdot {}^l k_{-1} / k_{-1}}{1 + {}^l k_2 / k_{-1}}$
Michaelis-Menten enzyme catalysis	$\text{Q} \xrightleftharpoons[k_{-1}]{k_1 [E_{free}]} \text{EQ} \xrightarrow{k_2} \text{P}$	$-\frac{d[\text{Q}]}{dt} = \frac{d[\text{P}]}{dt} = k_2 \cdot [EQ]$	$k_{app}$ $(a) = \frac{k_1 \cdot k_2 \cdot [E_{free}]}{k_{-1} + k_2}$ $(b) = \frac{k_2 \cdot [E_{tot}]}{(k_{-1} + k_2) / k_1 + [Q]} = \frac{V_{max}}{K_M + [Q]}$ $V_{max} = k_2 \cdot [E_{tot}]$ $K_M = (k_{-1} + k_2) / k_1$	$\frac{d[\text{Q}]}{d[\text{Q}]}$ $= \frac{{}^l k_1 \cdot {}^l k_2}{{}^h k_1 \cdot {}^h k_2} \cdot \frac{{}^h k_{-1} + {}^h k_2}{{}^l k_{-1} + {}^l k_2} \cdot \frac{[\text{Q}]}{[\text{Q}]}$ $= \frac{{}^l k_2}{\left( \frac{{}^h k_{-1} + {}^h k_2}{{}^h k_2} \right) / \frac{{}^l k_1}{{}^h k_1} \cdot \frac{[\text{Q}]}{[\text{Q}]}} = \frac{{}^l (V_{max} / K_M)}{{}^h (V_{max} / K_M)}$ <p>(see column to the left)</p>	$AKIE = \frac{EIE_1 \cdot KIE_2 + KIE_1 \cdot {}^l k_2 / k_{-1}}{1 + {}^l k_2 / k_{-1}}$ <p>(in analogy to above)</p>

between Q and I,  $EIE_1$ , so that their overall contribution is  $EIE_1KIE_2$ .

The terms  $k_{-1}/(k_{-1} + k_2)$  and  $k_2/(k_{-1} + k_2)$  can therefore be interpreted as probabilities of back reaction of I (or back flux)

$$p_{-1} = k_{-1}/(k_{-1} + k_2) \quad (28)$$

and of onward reaction of I (or forward flux)

$$p_2 = (1 - p_{-1}) = k_2/(k_{-1} + k_2) \quad (29)$$

so that eqn (25) can be rewritten as

$$AKIE = p_{-1} \cdot (EIE_1KIE_2) + p_2 \cdot KIE_1 \quad (30)$$

An analogous expression for fractionation factors is

$$\alpha_{\text{apparent}} = p_{-1} \cdot (\alpha_1^{\text{equ}} \alpha_2^{\text{equ}}) + p_2 \cdot \alpha_1^{\text{kin}} \quad (31)$$

and for enrichment factors

$$\begin{aligned} \varepsilon_{\text{apparent}} &= \alpha_{\text{apparent}} - 1 \\ &= [p_{-1} \cdot (\alpha_1^{\text{equ}} \alpha_2^{\text{equ}}) + p_2 \cdot \alpha_1^{\text{kin}}] - 1 \\ &= [p_{-1} \cdot (\varepsilon_1^{\text{equ}} + 1)(\varepsilon_2^{\text{equ}} + 1) + p_2 \cdot (\varepsilon_1^{\text{kin}} + 1)] - 1 \\ &= [p_{-1} \cdot (\varepsilon_1^{\text{equ}} \cdot \varepsilon_2^{\text{equ}} + \varepsilon_1^{\text{equ}} + \varepsilon_2^{\text{equ}} + 1) + p_2 \cdot (\varepsilon_1^{\text{kin}} + 1)] - 1 \quad (32) \\ &\approx [p_{-1} \cdot (\varepsilon_1^{\text{equ}} + \varepsilon_2^{\text{equ}} + 1) + p_2 \cdot (\varepsilon_1^{\text{kin}} + 1)] - 1 \\ &= [p_{-1} \cdot (\varepsilon_1^{\text{equ}} + \varepsilon_2^{\text{equ}}) + p_2 \cdot \varepsilon_1^{\text{kin}}] + (p_{-1} + p_2 - 1) \\ &= p_{-1} \cdot (\varepsilon_1^{\text{equ}} + \varepsilon_2^{\text{equ}}) + p_2 \cdot \varepsilon_1^{\text{kin}} \end{aligned}$$

where the combined probability of forward and back reaction is one (*i.e.*,  $p_{-1} + p_2 = 1$ ). Yet a different expression for values of  $\varepsilon$  may be obtained when taking into account that equilibrium isotope effects are composed of the kinetic isotope effects of forward and back reaction

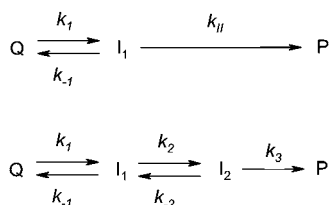
$$\varepsilon_f^{\text{equ}} = \varepsilon_f^{\text{kin}} - \varepsilon_{-f}^{\text{kin}} \quad (26)$$

so that

$$\begin{aligned} \varepsilon_{\text{apparent}} &= p_{-1} \cdot (\varepsilon_1^{\text{equ}} + \varepsilon_2^{\text{kin}}) + p_2 \cdot (\varepsilon_1^{\text{kin}}) \\ &= p_{-1} \cdot (\varepsilon_1^{\text{kin}} - \varepsilon_{-1}^{\text{kin}} + \varepsilon_2^{\text{kin}}) + p_2 \cdot (\varepsilon_1^{\text{kin}}) \quad (33) \\ &= \varepsilon_1^{\text{kin}} \cdot (p_{-1} + p_2) + (\varepsilon_2^{\text{kin}} - \varepsilon_{-1}^{\text{kin}}) \cdot p_{-1} \\ &= \varepsilon_1^{\text{kin}} + (\varepsilon_2^{\text{kin}} - \varepsilon_{-1}^{\text{kin}}) \cdot p_{-1} \end{aligned}$$

Expressions like eqn (33) are commonly found in geochemistry, whereas in organic (bio)chemistry expressions in the form of eqn (27) are preferred.

**Processes involving more steps.** This treatment is easily expanded to a three-step reaction when considering the second step as composed of two substeps:



giving

$$\begin{aligned} AKIE &= p_{-1} \cdot (EIE_1[p_{-2} \cdot (EIE_2KIE_3) + p_3 \cdot KIE_2]) + p_2 \cdot KIE_1 \\ &= p_{-1} \cdot p_{-2} \cdot (EIE_1EIE_2KIE_3) \\ &\quad + p_{-1} \cdot p_3 \cdot EIE_1 \cdot KIE_2 + p_2 \cdot KIE_1 \quad (34) \end{aligned}$$

The analogous equation for fractionation factors is

$$\alpha_{\text{apparent}} = p_{-1} \cdot p_{-2} \cdot (\alpha_1^{\text{equ}} \alpha_2^{\text{equ}} \alpha_3^{\text{kin}}) + p_{-1} \cdot p_3 \cdot \alpha_1^{\text{equ}} \alpha_2^{\text{kin}} + p_2 \cdot \alpha_1^{\text{kin}} \quad (35)$$

and for enrichment factors

$$\begin{aligned} \varepsilon_{\text{apparent}} &\approx p_{-1} \cdot p_{-2} \cdot (\varepsilon_1^{\text{equ}} + \varepsilon_2^{\text{equ}} + \varepsilon_3^{\text{kin}}) \\ &\quad + p_{-1} \cdot p_3 \cdot (\varepsilon_1^{\text{equ}} + \varepsilon_2^{\text{kin}}) + p_2 \cdot (\varepsilon_1^{\text{kin}}) \quad (36) \end{aligned}$$

$$\varepsilon_{\text{apparent}} \approx \varepsilon_1^{\text{kin}} + (\varepsilon_2^{\text{kin}} - \varepsilon_{-1}^{\text{kin}}) \cdot (p_{-1}) + (\varepsilon_3^{\text{kin}} - \varepsilon_{-2}^{\text{kin}}) \cdot (p_{-1} \cdot p_{-2}) \quad (37)$$

The corresponding expression in terms of rate constants, finally, is

$$AKIE = \frac{EIE_1EIE_2KIE_3 + EIE_1KIE_2 \cdot \frac{k_3}{k_{-2}} + KIE_1 \frac{k_2}{k_{-1}} \cdot \frac{k_3}{k_{-2}}}{1 + \frac{k_3}{k_{-2}} + \frac{k_2}{k_{-1}} \cdot \frac{k_3}{k_{-2}}} \quad (38)$$

It is easily seen that this concept can be expanded to include any number of further steps in multistep processes.

#### What governs the probabilities of onward and back reaction?

The question arises what factors determine the weight with which the respective steps enter in the calculation of  $AKIE$ . This can be illustrated for the case of a two-step reaction.

$$\begin{aligned} AKIE &= \frac{(EIE_1KIE_2) + \frac{k_2}{k_{-1}} \cdot KIE_1}{1 + \frac{k_2}{k_{-1}}} \\ &= \frac{\frac{k_{-1}}{k_1} \cdot \frac{1}{k_2} \cdot (EIE_1KIE_2) + \frac{1}{k_1} \cdot KIE_1}{\frac{k_{-1}}{k_1} \cdot \frac{1}{k_2} + \frac{1}{k_1}} \quad (27) \end{aligned}$$

Using the Arrhenius equation (eqn (6)) to express the rate constants  $k_i$

$$k_1 = A_1 \cdot \exp\{-(\Delta G_{TS1} - \Delta G_Q)/RT\} \quad (39)$$

$$k_2 = A_2 \cdot \exp\{-(\Delta G_{TS2} - \Delta G_{\text{Intermediate}1})/RT\} \quad (40)$$

and giving the equilibrium constant ( $k_1/k_{-1}$ ) as

$$\frac{k_1}{k_{-1}} = K_1 = \exp\{-(\Delta G_{\text{Intermediate}1} - \Delta G_Q)/RT\} \quad (41)$$

so that

$$\begin{aligned} \left(\frac{k_{-1}}{k_1} \cdot \frac{1}{k_2}\right) &= \exp\{(\Delta G_{\text{Intermediate}1} - \Delta G_Q)/RT\} \cdot \\ &\quad \frac{1}{A_2} \cdot \exp\{(\Delta G_{TS2} - \Delta G_{\text{Intermediate}1})/RT\} \\ &= \frac{1}{A_2} \cdot \exp\{(\Delta G_{TS2} - \Delta G_Q)/RT\} \quad (42) \end{aligned}$$



the following expression is obtained:

$AKIE =$

$$\frac{EIE_1 KIE_2 \cdot \left( \frac{1}{A_2} \cdot e^{\left( \frac{(\Delta G_{TS2} - \Delta G_Q)}{R \cdot T} \right)} \right) + KIE_1 \cdot \left( \frac{1}{A_1} \cdot e^{\left( \frac{(\Delta G_{TS1} - \Delta G_Q)}{R \cdot T} \right)} \right)}{1/A_2 \cdot e^{\left( \frac{(\Delta G_{TS2} - \Delta G_Q)}{R \cdot T} \right)} + 1/A_1 \cdot e^{\left( \frac{(\Delta G_{TS1} - \Delta G_Q)}{R \cdot T} \right)}} \quad (43)$$

In other words, the weight of the respective contributions is given by the energy difference between the transition state of the respective step  $i$  and the original contaminant  $Q$ , largely irrespective of any intermediates in between!

A similar consideration can be made for the isotope effect contributions. As illustrated in Fig. 1,  $KIE_1$  is determined by the energy differences between the isotopologues of reactant  $Q$ ,  $\Delta(\Delta G_Q)$ , and of transition state 1,  $\Delta(\Delta G_{TS1})$ :

$$KIE_1 = \frac{I A_1}{h A_1} \cdot \exp \left\{ - [\Delta(\Delta G_{TS1}) - \Delta(\Delta G_Q)] / RT \right\} \quad (44)$$

$EIE_1 KIE_2$ , on the other hand, is the product of  $EIE_1$  and  $KIE_2$  and is, therefore, determined by the energy differences between the isotopologues of reactant  $Q$ ,  $\Delta(\Delta G_Q)$ , and of transition state 2,  $\Delta(\Delta G_{TS2})$ :

$$\begin{aligned} EIE_1 KIE_2 &= \exp \left\{ - [\Delta(\Delta G_{Intermediate\ 1}) - \Delta(\Delta G_Q)] / RT \right\} \\ &\cdot \frac{I A_2}{h A_2} \cdot \exp \left\{ - [\Delta(\Delta G_{TS2}) - \Delta(\Delta G_{Intermediate\ 1})] / RT \right\} \\ &= \frac{I A_2}{h A_2} \cdot \exp \left\{ - [\Delta(\Delta G_{TS2}) - \Delta(\Delta G_Q)] / RT \right\} \quad (45) \end{aligned}$$

In other words, it is not necessary to spell out the isotope effect contributions as products of equilibrium and kinetic isotope effects. Alternatively, these contributions may again be thought to arise from the difference in isotopologue energies between transition state  $i$  and original contaminant  $Q$ , largely independent of any intermediates in between!

Similar expressions can be derived for processes involving any number of steps. This conceptual understanding makes it possible to reduce a commonly rather complicated mathematical framework to a very simple picture, as illustrated for the following case of a hypothetical six-step reaction (Fig. 6).

The observable isotope fractionation stems from the steps with the highest activation energy. In the case of Fig. 6 they are 5, 3, 1 and 6. In comparison, the contribution of steps 2 and 4 is negligible because activation energies are much smaller. In other words, isotope fractionation during multistep reactions reflects the rate-determining steps, or “bottlenecks” of the overall cascade.<sup>106,108</sup> Of these rate-determining steps, only steps 3 and 6 contribute significant isotope effects. In contrast – as indicated by the arrows in Fig. 6 – the energy difference between the isotopologues in the transition states 1 and 5 is similar to that of the original reactant  $Q$  so that no isotope effects result. Taken together, the observable isotope fractionation  $AKIE$  will be a weighted average of the four steps and will, therefore, be significantly reduced (= “masked”) compared to the  $KIE$  of steps 3 and 6. The following picture emerges.

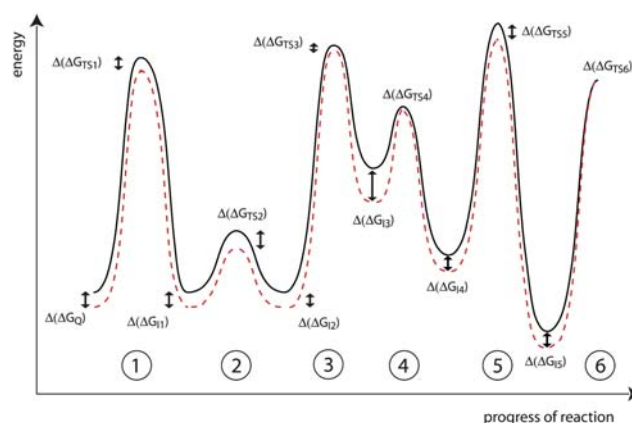


**Fig. 6** Activation energies during a hypothetical six-step reaction. The solid line indicates light isotopologues, the dashed line heavy isotopologues. Energy differences between the isotopologues in each reactant state and transition state are given by arrows.

(1) Isotope fractionation in multistep processes is dominated by the contribution from the bottlenecks, or rate-determining steps.

(2) If such rate-determining steps show very small isotope fractionation, the intrinsic isotope effect of the irreversible chemical bond conversion (e.g., in step 6) will become smaller (i.e., be masked) in the observable  $AKIE$  value.

(3) If several steps are rate-determining, their isotope fractionation enters with a similar weight so that more than one step can dominate.

(4) If several of these steps show isotope effects, also isotope fractionation in the  $AKIE$  value may stem from more than one step,<sup>106,109</sup> e.g., steps 3 and 6 in Fig. 6.

**Possible transformation steps in natural processes.** Not all natural process steps are first-order chemical reactions as considered above. The question arises whether the same treatment applies also to other processes like zero-order transformations, reactions of higher reaction order, or mass transfer. Table 2 and 3 summarize the respective equations. They demonstrate that also these processes may be integrated into the conceptual treatment when substituting  $k_i$  and  $KIE_i$  with the expressions of  $k$  and  $AKIE$  given in the tables in a similar way as done in eqn (34).

**Expressions for multistep transformations from the literature. Biochemistry.** In the biochemical literature it is commonly assumed that only one step of a reaction cascade is associated with an isotope effect (for example step 3) so that the expression

$$AKIE = \frac{EIE_1 EIE_2 KIE_3 + EIE_1 KIE_2 \cdot \frac{k_3}{k_{-2}} + KIE_1 \frac{k_2}{k_{-1}} \cdot \frac{k_3}{k_{-2}}}{1 + \frac{k_3}{k_{-2}} + \frac{k_2}{k_{-1}} \cdot \frac{k_3}{k_{-2}}} \quad (38)$$

simplifies to

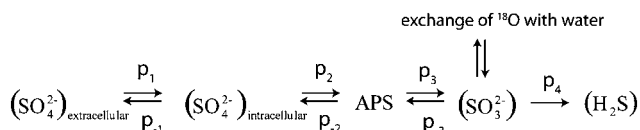
$$AKIE = \frac{KIE_3 + \frac{k_3}{k_{-2}} + \frac{k_2}{k_{-1}} \cdot \frac{k_3}{k_{-2}}}{1 + \frac{k_3}{k_{-2}} + \frac{k_2}{k_{-1}} \cdot \frac{k_3}{k_{-2}}} = \frac{KIE_3 + c}{1 + c} \quad (46)$$

The lumped rate constant terms are commonly called “commitment to catalysis  $c$ ” and  $AKIE$  is often interpreted as kinetic isotope effect on the Michaelis–Menten parameters,  $^l(V_{\max}/K_M)^h(V_{\max}/K_M)$  (see Table 3) so that the equivalent expression found in the literature is<sup>103,110</sup>

$$\frac{^l(V_{\max}/K_M)}{^h(V_{\max}/K_M)} = \frac{(^l k_3/^h k_3)_{\text{intrinsic}} + c}{1 + c} \quad (47)$$

The more committed an enzyme is – meaning that the bond conversion step with  $k_3$  has a low activation energy and is very fast and efficient – the greater is the term “ $c$ ” so that the intrinsic isotope effect is masked. Dedicated studies with multiple labeling techniques have made it possible to resolve for selected enzyme reactions the kinetics and isotope effects of essentially all important steps providing a superb process understanding in exemplary cases.<sup>63,65,103,111</sup> This insight illustrates (i) that even on the level of enzymatic reactions the intrinsic  $KIE$  may already be masked in the observable  $AKIE$ , and (ii) that this effect tends to become greater if enzymes have made the intrinsic bond conversion more efficient.

**Organic Geochemistry 1: Sulfate Reduction.** In a similar way as isotope analysis of  $^{13}\text{C}/^{12}\text{C}$  may be used to quantify the transformation of organic contaminants (see Part I), fractionation of  $^{34}\text{S}/^{32}\text{S}$  in sulfate offers the potential to quantify natural sulfate reduction and has been intensely studied in geochemistry. The conceptual picture is that extracellular sulfate gets into the cell, is converted to adenosine-5'-phosphosulfate (APS), reduced to sulfite and undergoes several imperfectly understood reduction processes until sulfide is formed and leaves the cell again.



Rees<sup>100</sup> was the first to provide a mathematical framework

$$\begin{aligned} \alpha_{ae} &\approx \alpha_{ab} + (\alpha_{bc} - \alpha_{ba}) \cdot X_b \\ &+ (\alpha_{cd} - \alpha_{cb}) \cdot X_b \cdot X_c + (\alpha_{de} - \alpha_{dc}) \cdot X_b \cdot X_c \cdot X_d \end{aligned} \quad (48)$$

which is equivalent to eqn (37) when expressed as a four-step reaction:

$$\begin{aligned} \varepsilon_{\text{apparent}} &\approx \varepsilon_1^{\text{kin}} + (\varepsilon_2^{\text{kin}} - \varepsilon_{-1}^{\text{kin}}) \cdot (p_{-1}) \\ &+ (\varepsilon_3^{\text{kin}} - \varepsilon_{-2}^{\text{kin}}) \cdot (p_{-1} \cdot p_{-2}) + (\varepsilon_4^{\text{kin}} - \varepsilon_{-3}^{\text{kin}}) \cdot (p_{-1} \cdot p_{-2} \cdot p_{-3}) \end{aligned} \quad (49)$$

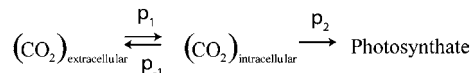
The difference is that Rees expressed the kinetic enrichment factors as  $\alpha$  values (unlike in the nomenclature of today) and called the probabilities  $p_i$  fluxes  $X_i$ .

In numerous studies, sulfur isotope fractionation has since been found to be highly variable, with  $\varepsilon_{\text{apparent}}$  values ranging between 0‰ and up to  $-47\text{‰}$ <sup>78,112</sup>. Such variable fractionation has been explained by the fact that different steps may become the bottleneck of the multistep transformation. For example, if the first step is already irreversible,  $\varepsilon_{\text{apparent}}$  is very small. In contrast, if the bottleneck is at the end of the cascade, more equilibrium and kinetic isotope effects can contribute to the overall fractionation so that  $\varepsilon_{\text{apparent}}$  becomes greater.<sup>78,100</sup>

A direct experimental confirmation of this model has been achieved by measuring not only the isotope value of  $^{34}\text{S}/^{32}\text{S}$ , but also of  $^{18}\text{O}/^{16}\text{O}$  in sulfate.<sup>78,112,113</sup> The reason is that this oxygen exchanges with  $^{18}\text{O}$  in water at the stage of the intermediate sulfite,  $\text{SO}_3^{2-}$ , but not at the stage of sulfate,  $\text{SO}_4^{2-}$ . An exchange of  $^{18}\text{O}$  is therefore only observed in sulfate if the first steps of the cascade are reversible meaning that the intermediate sulfite is reoxidized back to sulfate. By measuring  $^{18}\text{O}$  in sulfate, the parameter  $(p_{-1} \cdot p_{-2} \cdot p_{-3})$  becomes therefore directly accessible from experiments! Recent studies have confirmed that  $^{34}\text{S}/^{32}\text{S}$  fractionation in sulfate was significantly higher under circumstances where also exchange of  $^{18}\text{O}$  took place.<sup>112–114</sup> This example illustrates that although variable  $\varepsilon$  values arising from multistep reactions can complicate the quantification of natural transformation, they provide, on the other hand, the key to a true process understanding.

**Organic Geochemistry 2: Photosynthesis.** Carbon isotope fractionation during photosynthesis is the textbook example for a multistep reaction and is of enormous importance in many fields.<sup>102,104</sup> For example, the difference in fractionation between  $\text{C}_3$  and  $\text{C}_4$  plants creates distinct  $^{13}\text{C}$  input signals that can be used to reconstruct past vegetation, or to trace carbon fluxes in ecological food webs.

$\text{C}_3$  plants. Photosynthesis in  $\text{C}_3$  plants may be regarded as a two-step process.  $\text{CO}_2$  diffuses more or less freely in and out of the cell (step 1) and is subsequently converted in the photosynthesis reaction (step 2):



The expression derived for this process is<sup>102,104</sup>

$$\Delta \approx a + (b - a) \cdot \left[ \frac{[\text{CO}_2]_{\text{intracellular}}}{[\text{CO}_2]_{\text{extracellular}}} \right] \quad (50)$$

which is again equivalent to eqn (33):

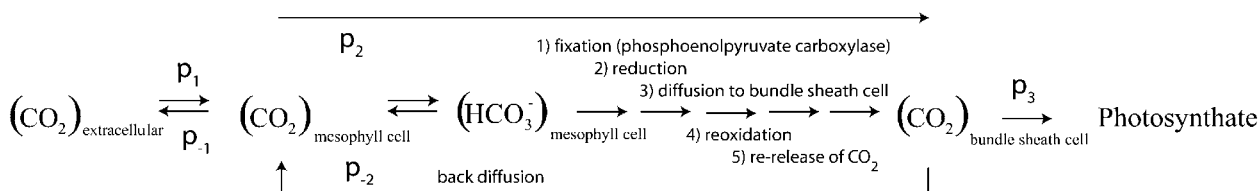
$$\varepsilon_{\text{apparent}} \approx \varepsilon_1^{\text{kin}} + (\varepsilon_2^{\text{kin}} - \varepsilon_{-1}^{\text{kin}}) \cdot (p_{-1}) \quad (33)$$

Therefore, similar as in the case of sulfate reduction, the probability of the back reaction is linked to an experimental parameter, in this case  $[\text{CO}_2]_{\text{intracellular}}/[\text{CO}_2]_{\text{extracellular}}$ . Since  $\text{CO}_2$  is consumed inside the cell, a concentration gradient builds up to the outside. This gradient is steeper if the cell wall is less permeable and back diffusion is small (*i.e.*,  $[\text{CO}_2]_{\text{intracellular}} \ll [\text{CO}_2]_{\text{extracellular}}$  and  $p_{-1} \ll 1$ ). In such a case, also  $\varepsilon_{\text{apparent}}$  is small because the first step is rate-determining, and isotope fractionation of the much stronger fractionating second step is masked ( $\varepsilon_2 \approx -29\text{‰}$ ,  $\varepsilon_1 \approx -4.4\text{‰}$ ).<sup>102</sup> Because this also means that the plant loses less water, the magnitude of isotope fractionation in  $\text{C}_3$  plants has been linked to water use efficiency.<sup>102</sup> Typical values for  $\varepsilon_{\text{apparent}}$  in  $\text{C}_3$  plants are around  $-20\text{‰}$ .

$\text{C}_4$  plants. Photosynthesis in  $\text{C}_4$  plants, in contrast, is best described as per the scheme of Table 4.<sup>105</sup>

$\text{C}_4$  plants have an additional preconcentration step:  $\text{CO}_2$  is transported from one type of cells (mesophyll cell) to another (bundle sheath cell) in order to increase the  $\text{CO}_2$  concentration close to the site of photosynthesis (Step 2). This is a strategy to

Table 4



Parameter	Meaning of the carbon isotopic enrichment factor	Equivalent parameter of eqn (37)
$\varepsilon_{P4}$	observable kinetic enrichment factor in $\text{C}_4$ plants	$\varepsilon_{\text{apparent}}$
$\varepsilon_{ta}$	kinetic enrichment factor for diffusion of $\text{CO}_2$ in air	$\varepsilon_1, \varepsilon_{-1}$
$\varepsilon_{tw}$	kinetic enrichment factor for diffusion of $\text{CO}_2$ in water	$\varepsilon_{-2}$
$\varepsilon_c$	kinetic enrichment factor for fixation of $\text{HCO}_3^-$ by phosphoenolpyruvate carboxylase	
$\varepsilon_{bld}$	equilibrium enrichment factor relating $\text{HCO}_3^-$ and dissolved $\text{CO}_2$	
$(\varepsilon_c - \varepsilon_{bld})$	composite kinetic enrichment factor for the second step	$\varepsilon_2$
$\varepsilon_f$	kinetic enrichment factor of the photosynthesis reaction	$\varepsilon_3$
$(1 - f_2)$	probability of back diffusion of $\text{CO}_2$ out of the cell in step 1	$p_{-1}$
$L$	"leaching parameter" denoting the probability of $\text{CO}_2$ back diffusion from bundle sheath cell to the mesophyll cell in step 2	$p_{-2}$

enable photosynthesis under conditions where diffusion through the cell wall must be minimized in order not to lose water. For this process Hayes<sup>105</sup> derived the expression

$$\varepsilon_{P4} = \varepsilon_{ta} + [\varepsilon_c - \varepsilon_{bld} + L(\varepsilon_f - \varepsilon_{tw}) - \varepsilon_{ta}] \cdot (1 - f_2) \quad (51)$$

where the parameters have the meaning summarized in Table 4. The expression may be rewritten as

$$\begin{aligned} \varepsilon_{\text{apparent}} &= \varepsilon_1^{\text{kin}} + [\varepsilon_2^{\text{kin}} + L(\varepsilon_3^{\text{kin}} - \varepsilon_{-2}^{\text{kin}}) - \varepsilon_{-1}^{\text{kin}}] \cdot (1 - f_2) \\ &= \varepsilon_1^{\text{kin}} + [\varepsilon_2^{\text{kin}} - \varepsilon_{-1}^{\text{kin}}] \cdot (1 - f_2) + (\varepsilon_3^{\text{kin}} - \varepsilon_{-2}^{\text{kin}}) \cdot (1 - f_2) \cdot L \end{aligned} \quad (52)$$

which is again the general expression for a three step reaction

$$\varepsilon_{\text{apparent}} \approx \varepsilon_1^{\text{kin}} + (\varepsilon_2^{\text{kin}} - \varepsilon_{-1}^{\text{kin}}) \cdot (p_{-1}) + (\varepsilon_3^{\text{kin}} - \varepsilon_{-2}^{\text{kin}}) \cdot (p_{-1} \cdot p_{-2}) \quad (37)$$

Fractionation in  $\text{C}_4$  plants is generally much smaller than in  $\text{C}_3$  plants (around  $\varepsilon_{\text{apparent}} \approx -5\text{‰}$ ). As laid out by Hayes, this has two reasons. (a) Diffusion in step 1 is more hindered than in  $\text{C}_3$  plants. (b) In addition, the lumped kinetic isotope fractionation  $(\varepsilon_c - \varepsilon_{bld}) = \varepsilon_2$  of the second step is *inverse*, because bicarbonate is enriched in  $^{13}\text{C}$  compared to  $\text{CO}_2$ . This preference for heavy isotopes in step 2 greatly reduces the overall preference for light isotopes in  $\varepsilon_{\text{apparent}}$ . In fact, depending on the parameters of  $p_{-1}$  and  $p_{-2}$ ,  $\varepsilon_{\text{apparent}}$  may even become inverse! This example shows that a process understanding is important to conceptualize observable isotope fractionation, because a different process (e.g., step 2) may be observed in the apparent fractionation than expected (i.e., step 3)!

**Importance of different steps during environmental contaminant transformation.** Analogous effects as conceptualized in these classical studies have also been observed for multistep transformations of organic contaminants. In particular, the intrinsic isotope effect of a given (bio)chemical transformation mechanism is not always observed in natural biodegradation reactions.<sup>25</sup> Isotope fractionation was even negligible in some cases of aerobic MTBE degradation,<sup>91</sup> reductive chlorinated ethylene

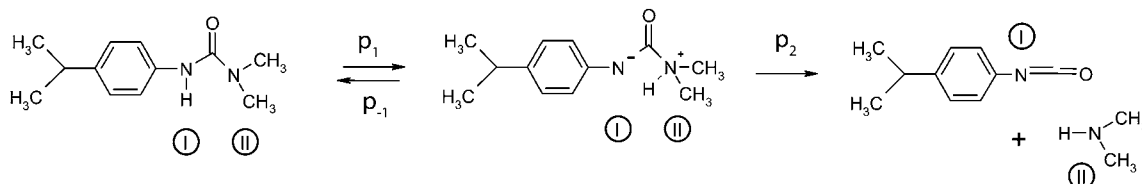
transformation<sup>115–118</sup> or isoproturon demethylation<sup>88</sup> where, according to the mechanistic picture, substantial isotope effects would be expected. The following section sheds further light on the relevance of the different steps in Fig. 5 by discussing important case studies of multistep reactions of organic contaminant transformations.

**Mass transfer into the cell.** Recent studies<sup>83,115–117</sup> hypothesized that mass transfer into the cell of bacteria may become a bottleneck to degradation. Reductive dechlorination of tetrachloroethylene (PCE) and trichloroethylene (TCE) was investigated by different microbial strains, in cell-free extracts and by pure cobalamine (this is the cofactor present in most reductive dehalogenases).<sup>115–117</sup> A trend of increasing isotope fractionation with decreasing cell integrity indicated that uptake or transport into the cell may be rate determining. A similar hypothesis was brought forward in a study of toluene biodegradation under iron reducing conditions. Smaller isotope fractionation was observed when the microorganisms were attached to solid iron(III) phases than when they were provided with dissolved Fe(III) in solution.<sup>83</sup> Hence it was postulated that mass transfer of toluene into the cell became rate-determining when the microbes were attached to the solid iron(III) phases.

**Commitment to catalysis in enzyme reactions.** In the case of toluene degradation by *Pseudomonas* mt-2 isotope fractionation could directly be linked to enzyme activity. The organism had been shown to form a less active apoenzyme when grown under conditions of iron-deficiency.<sup>119</sup> Carbon and hydrogen isotope fractionation in toluene was measured under such conditions of iron limitation, and was found to be significantly greater than in the presence of iron.<sup>81</sup> It was therefore concluded that only the apoenzyme made it possible to observe the intrinsic isotope effect of the toluene transformation. In contrast, a normally functioning enzyme is to a greater extent committed meaning that the intrinsic isotope effect is to some extent masked.

**Dissolution of contaminants from an organic phase.** Also partitioning, or dissolution, of contaminants from an organic phase into water can become the bottleneck of a natural transformation. A recent study has simulated such a scenario by

measuring the carbon isotope fractionation during microbial TCE degradation under conditions where TCE was slowly released from a pure tetradecane phase.<sup>120</sup> Significantly smaller



isotope fractionation was observed in the presence of the tetradecane phase than in its absence. This result has implications for organic contaminants such as polycyclic aromatic hydrocarbons, which sorb strongly and may be trapped in naturally occurring organic matter so that they are not readily bioavailable. This aspect will be taken up again.

When a contaminant dissolves from its own pure phase, however, this would generally not be expected to be a bottleneck for natural biodegradation – concentrations close to the pure phase are normally so high that they do not limit microbial degradation. If any, freshly dissolved contaminant can mix into water parcels that have already undergone some degradation so that degradation-induced changes in isotope values are diluted out<sup>121</sup> and degradation will be underestimated<sup>50,51,53</sup>. As briefly mentioned in the discussion of field applications earlier, this effect is caused by hydrological mixing rather than by bottlenecks in multistep processes.

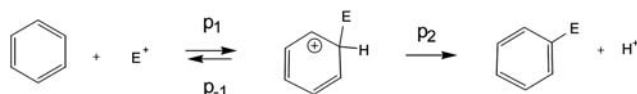
**Effect of masking on quantification and mechanistic elucidation – the importance of dual isotope plots.** Masking can complicate the interpretation of isotope fractionation. Values of  $\epsilon$ , or  $\alpha$ , can be highly variable even for the same transformation mechanism raising the question which number should be used to quantify natural biodegradation. Estimates are best given as possible ranges, and for conservative estimates the greatest  $\epsilon$  reported should be used.<sup>15</sup> In addition, masking can complicate the mechanistic interpretation of  $\epsilon$  values in terms of kinetic isotope effects (see above), because numbers may be much smaller than expected for a given mechanistic scenario. A solution to this problem is offered by dual isotope plots. As in the examples above, masking of isotope fractionation is generally caused by non-fractionating steps. Such non-fractionating steps mask isotope fractionation of both elements to the same extent so that dual isotope slopes remain the same.<sup>81,83</sup> Therefore, dual isotope slopes can be used to discern the underlying mechanism even in the presence of masking!

**Variable dual isotope slopes in (bio)chemical multistep reactions.** As indicated in the sketch of Fig. 6, however, transformation processes may entail several steps which cause isotope fractionation (e.g., the photosynthesis of  $C_4$  plants discussed above). Recent examples of pollutant transformation reactions stem from nitroaromatic compound reduction<sup>86</sup> or from abiotic hydrolysis of isoproturon at 60 °C.<sup>87</sup> This has important consequences, because dual isotope slopes are no longer constant, but may change depending on the nature of the rate-determining step. This will be illustrated in greater detail using the isoproturon example.

The abiotic hydrolysis of isoproturon involves an intramolecular proton transfer followed by decomposition according to the following scheme:

The first step is catalyzed by the presence of buffers so that, depending on pH and the presence of anions, either step may become rate-determining. A dedicated fragment-specific isotope analysis of isoproturon has made it possible to measure isotope effects at each of the nitrogen atoms separately ((I) and (II)).<sup>87,122</sup> In contrast to more evenly distributed carbon isotope effects, it was found that isotope effects at the nitrogen atom (I) occurred mostly in the first step, while isotope effects at the nitrogen atom (II) occurred mostly in the second step. Therefore, when dual isotope slopes (C versus N) were derived for each fragment, these slopes were actually not constant, but varied depending on the rate-determining step!<sup>87</sup> A textbook example of such variations in dual isotope slopes is also the fractionation of  $^2H$  versus  $^{18}O$  in precipitation: while the dual isotope slope follows the meteoric water line in the case of equilibrium isotope fractionation, shallower slopes indicate the effect of diffusion-controlled evaporation.<sup>123</sup>

Therefore, although differences in dual isotope slopes are in most cases a strong indicator for different mechanisms, and are typically not affected by masking, care must be taken in multistep reactions when more than one step can cause fractionation. Of concern are in particular (bio)chemical transformations that involve short-lived intermediates so that already subtle variations in reaction conditions may lead to shifts. Potential examples are ester or amide hydrolysis such as in the case of isoproturon,<sup>87,124</sup> electron transfer reactions<sup>86,125</sup> or electrophilic aromatic substitutions. The latter reaction has been hypothesized as possible mechanistic scenario for the initial activation step of anaerobic benzene degradation:<sup>80</sup>



The electrophile E attacks the aromatic ring and forms a short lived intermediate before  $H^+$  is eliminated. Carbon isotope effects are anticipated in both steps, but a primary hydrogen isotope effect is expected only in the second. Therefore, if subtle differences at the enzymatic site change the probabilities of forward and back reaction, it cannot be excluded that different dual isotope slopes result despite the fact that the same mechanism prevails!

**Linking isotope fractionation to bioavailability.** In particular, kinetics in a multistep process can shift if a specific step is accelerated by the presence of a cosubstrate, differences in pH<sup>126</sup> or the presence of a catalyst, such as a buffer in the case of abiotic isoproturon hydrolysis.<sup>87</sup> Recent work considered for the first time that also the concentration of free enzyme inside



microorganisms (*i.e.*, unoccupied by a substrate) can change.<sup>127</sup> Thullner, Kampara and coworkers demonstrated that observable isotope fractionation may become masked in such cases,<sup>127,128</sup> and that the degree of masking may even be linked to bioavailability.<sup>127–129</sup>

To this end, a situation as depicted in Fig. 7 was considered.<sup>130</sup> Although an organic contaminant is present in significant concentrations ( $(Q)_{aq}$ ) in bulk solution, it may become depleted in vicinity of the microorganism on the microscale. The reason is that microbial transformation is more quickly than mass transfer into micropores so that a gradient forms on the microscale. The bioavailable substrate concentration ( $(Q)_{bioavailable}$ ) that an organism “sees” is, hence, much smaller than the concentration ( $(Q)_{aq}$ ) which can be sampled in solution. Thullner and coworkers considered what happens under such conditions when contaminant concentrations ( $Q$ ) change from high to low.

At high concentrations of  $Q$  all enzymes are caught up in enzyme-substrate complexes (EQ). Very little free enzyme ( $E_{free}$ ) is left so that Michaelis–Menten kinetics is in the zero-order regime, the enzyme reaction runs at its limit and represents the bottleneck of the overall transformation. Under such conditions no appreciable concentration gradient builds up,  $Q$  is readily bioavailable, molecules of  $Q$  escape back into solution so that the isotope fractionation of the enzyme reaction is fully observable.

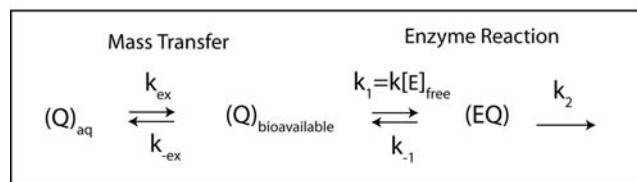
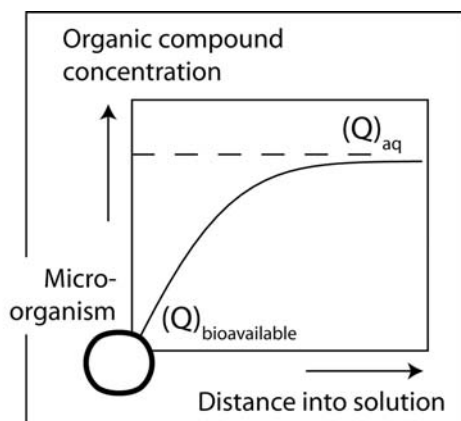


**Fig. 7** Theoretical framework to link bioavailability to observable isotope fractionation. Case A ( $Q$  is bioavailable): There is no concentration gradient between microorganism and bulk solution (dashed line). Almost all enzymes are engaged in (EQ) complexes and  $[E]_{free}$  is small. Consequently  $k_{ex} > k[E]_{free}$  and the isotope effect of the enzymatic reaction is observable. Case B ( $Q$  is little bioavailable): A concentration gradient builds up (solid line) and concentrations of  $Q$  are small in vicinity of the microorganism. More enzymes are therefore present in their free form  $[E]_{free}$ , and  $k[E]_{free} > k_{ex}$ . Consequently, the enzyme reaction is fast compared to mass transfer and the isotope effect of the enzymatic reaction is masked.

At low concentrations of  $Q$ , in contrast, less free enzyme is caught up as (EQ) so that more enzymes are present in their free form ( $E_{free}$ ). The Michaelis–Menten kinetics shifts to the first-order regime. The rate constant  $k_1$  becomes large compared to  $k_{ex}$ , and biotransformation becomes fast compared to mass transfer. Consequently, a concentration gradient builds up,  $Q$  is no longer bioavailable, molecules of  $Q$  cannot escape back into solution and the isotope fractionation of the enzyme reaction is suddenly masked.

Therefore, even if all other parameters during such a transformation reaction are held constant, the observable isotope fractionation may change nonetheless, just because the substrate concentration decreases! Toluene degradation experiments with resting cells verified that such a situation can indeed occur: smaller observable isotope fractionation was observed when toluene concentrations became smaller.<sup>128,129</sup> This insight has important consequences. (i) On the one hand, such a shift in kinetics may quite generally be expected for any type of catalyzed reaction. It leads to kinetic regimes where experimental data can no longer be evaluated according to the Rayleigh equation, because the isotope fractionation changes during the duration of the process. (ii) On the other hand, the treatment suggests that observable isotope fractionation can be used as a diagnostic tool to demonstrate that a substrate is *not* fully bioavailability-limited: otherwise molecules of  $Q$  would not diffuse back to solution to report the intrinsic isotope fractionation!

Taken together, the examples from recent studies show that isotope fractionation must be interpreted very carefully in natural multistep processes. Values of  $\epsilon$  can be smaller than anticipated, unexpected processes may be represented, dual isotope slopes can show variations for the same mechanism, and even an evaluation according to the Rayleigh equation may have to be adapted to different kinetic regimes. On the other hand, however, such variations bear enormous potential to learn something about the underlying processes. Isotope fractionation may give information about the commitment and type of enzymes involved, fractionation of important steps can be unmasked through systematic variation of reaction conditions, and isotope fractionation may potentially be linked even to substrate bioavailability.

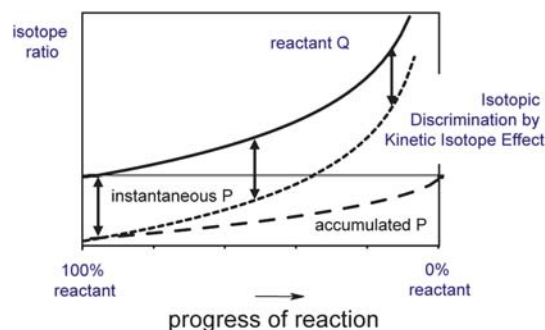


**Fig. 8** Evolution of isotope ratios of reactant  $Q$ , instantaneously formed product  $P$  and accumulated product  $P$  in the case of a normal kinetic isotope effect during an irreversible transformation in a closed reaction container.

#### IV. Isotope fractionation and product formation

Product formation is often not the primary focus of isotope fractionation studies. A reason is that evidence from isotope fractionation is frequently most valuable if *no* products are detected: the enrichment of stable isotopes in the remaining contaminants can provide an independent line of evidence for their natural degradation. If products can be detected, on the other hand, and if they are even amenable to compound specific isotope analysis, important additional information may be obtained. This section will discuss what type of information may be extracted, and will show that an understanding of product formation is in many cases important for a correct interpretation of observable isotope fractionation.

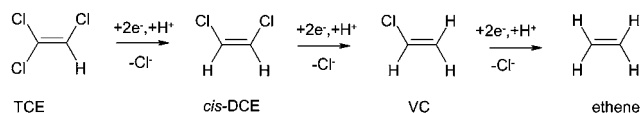
Fig. 8 illustrates the evolution of reactant and product isotope ratios during an irreversible reaction in a closed container. Due to the (normal) kinetic isotope effect associated with the transformation, the instantaneously formed product is at any time depleted in heavy isotopes compared to the reactant (arrows in Fig. 8). As a consequence, the reactant Q becomes increasingly enriched in heavy isotopes, whereas the *accumulated* product (the one that can be measured in a closed container) starts off with the characteristically depleted value and, for reasons of isotopic mass balance, ends up at the original value of Q. Therefore, if a putative product P is detected at a contaminated site, and if this product is depleted in heavy isotopes compared to its suspected precursor contaminant Q, isotope analysis may provide evidence that P is indeed formed as product of Q!

This mechanistic picture is accurate if a reaction has just one product and if this product does not react further. Generally, however, intermediates are formed which are subsequently further degraded, or products are formed in parallel reaction pathways. In such cases, the graph in Fig. 8 describes the *weighted average* of the isotope ratios of all products. Between each other, however, the products may show differences from this average. These differences reflect again important mechanistic information, for example about branching points in metabolic pathways. These aspects have been treated in seminal reviews about biosynthetic pathways of natural compounds.<sup>105,131</sup> Here, those facets will be discussed that are of immediate relevance for the interpretation of organic contaminant degradation.

**Products from reacting versus non-reacting positions.** For the interpretation of product isotope values a first important question is “What part of the molecule does the product come from?” If isotopes stem from non-reacting positions of the original contaminant, the isotope ratio of these positions remains unchanged irrespective of the fact that a reaction occurs in the rest of the molecule.<sup>90,132–134</sup> A particularly well-investigated example is the isotope ratio of *tert*-butyl alcohol (TBA). TBA is formed as product of MTBE degradation which – depending on geochemical conditions – may be even more persistent than the parent compound.<sup>135</sup> Since natural MTBE transformations involve the methoxy group rather than the *tert*-butyl group, (see Fig. 3 and Table 1) TBA isotope ratios are not expected to change in these transformations. Indeed, the carbon isotope ratio of TBA was demonstrated to be unaffected by the progress of microbial transformation, and contained even more <sup>13</sup>C than the original MTBE.<sup>134</sup> A comparison of TBA and MTBE isotope

ratios would, therefore, not establish meaningful precursor-product relationships. Instead, the isotope ratio of TBA offers potential for source fingerprinting, since it represents the conservative isotope ratio in the non-reactive part of MTBE.<sup>92,95</sup> This example demonstrates again that a mechanistic understanding is crucial for a correct interpretation of observable isotope ratios.

**Products as intermediates of sequential reactions.** In sequential reactions products are formed and consumed at the same time. An important example is the biodegradation of the groundwater contaminant trichloroethylene (TCE). *cis*-Dichloroethylene (*cis*-DCE) and vinyl chloride (VC) often accumulate as more problematic intermediates before they are further transformed to non-toxic ethene. The interpretation of their isotope ratios is therefore of great interest.



All carbon isotopes are quantitatively transferred from one compound to the other in this transformation sequence. (For chlorine isotopes the situation is different, however, see Hunkeler *et al.*<sup>90</sup>) Consequently, the instantaneous product reflects the characteristic isotopic discrimination similarly as in Fig. 8. In contrast to the one-step scenario of Fig. 8, however, *cis*-DCE and VC may be further degraded. Isotope ratios of these intermediates are, therefore, subject to two opposing forces: (a) An influx of molecules that are *depleted* in <sup>13</sup>C compared to the precursor compound, due to the kinetic isotope effect of the preceding transformation. This influx is strongest if the *precursor* gets transformed fast and if the associated isotope effect is great. (b) Reaction of the intermediate leading to an *enrichment* of <sup>13</sup>C. This effect is strongest if transformation of the *intermediate* is fast and the associated isotope effect large.

The resulting picture is that intermediates are initially depleted in <sup>13</sup>C compared to their precursor, but subsequently become enriched in <sup>13</sup>C when the influx becomes smaller and the effect of their own degradation kicks in. Numerous studies have investigated such isotope trends during chlorinated ethylene biodegradation. Illustrative examples are given by Hunkeler *et al.*,<sup>33,136</sup> Slater *et al.*,<sup>137</sup> Bloom *et al.*,<sup>138</sup> van Breukelen *et al.*<sup>139</sup> or Morill *et al.*<sup>35,121</sup> Intermediates may even become more enriched than their precursor,<sup>139</sup> for example if the isotope effect of the preceding transformation is very small. In general, however, it was observed that compounds remain depleted in <sup>13</sup>C compared to their direct precursor over the range of concentrations amenable to isotope analysis so that a picture similar to Fig. 9, left panel, is obtained.

At chlorinated ethylene-contaminated sites, finally, it is often not sufficient to show that biodegradation occurs, but it must be demonstrated that this biodegradation involves complete dehalogenation to non-problematic ethene. In principle, such a line of evidence can be provided by an isotopic mass balance of TCE, *cis*-DCE and VC. Isotope ratios of these compounds are weighted by their concentrations and added up. If this weighted average is the same as the original TCE isotope ratio at the

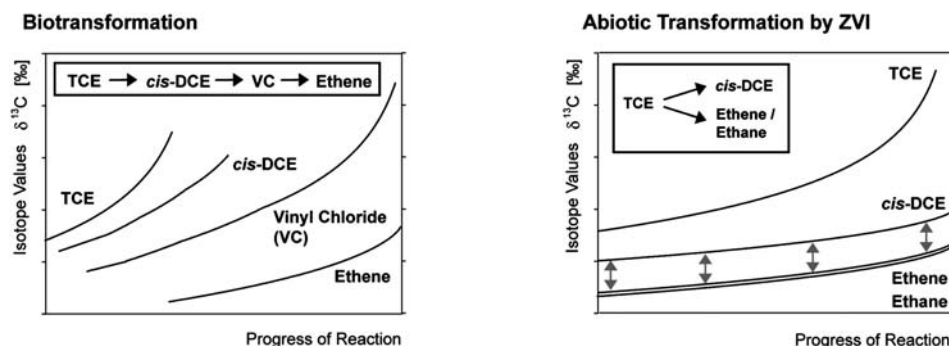
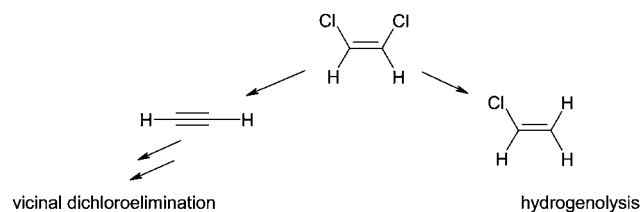


**Fig. 9** Evolution of carbon isotope ratios of chlorinated ethenes in biodegradation where products are formed in sequence (left) and in abiotic transformation by zero-valent iron, where they are formed in parallel (right).

source, then the isotopic mass balance is closed and there is no evidence for further degradation to ethene. In contrast, if the weighted average is more positive than the source value, this would indicate that light isotopes have “escaped” providing direct evidence for further transformation to ethene.<sup>140</sup> In practice, such assessments may be limited by the analytical accuracy of the *concentration* analysis, due to errors associated with sampling, storage, and other aspects of sampling handling (see, for example, Blessing *et al.*<sup>141</sup>).

The examples show that product isotope ratios in sequential reactions are determined by the interplay of reaction rates and associated isotope effects and are not easily predicted (see Fig. 9). Also here, interpretations of precursor-product isotope relationships must, therefore, be performed with caution.

**Products in parallel reactions.** Some contaminants may be transformed in reactions that occur in parallel so that several products are formed at the same time. An example is the reductive dehalogenation of chlorinated ethylenes by zero-valent metals where either a C–Cl bond is reduced to a C–H bond (hydrogenolysis), or two chlorine substituents are eliminated simultaneously (vicinal dichloroelimination). The first pathway forms more problematic intermediates, whereas the second quickly leads to non-toxic products.



Even though products and pathways are the same, this transformation may occur in two fundamentally different ways (see Fig. 10).

**Case A.** Two transformations are occurring independent of each other. Each is associated with its own specific isotopic enrichment factor  $\varepsilon_i$ . The observable isotope fractionation  $\varepsilon$  that can be measured in the reactant Q is a weighted average of both and will vary depending on the contribution of either transformation:

$$\varepsilon = F_{P1} \cdot \varepsilon_1 + F_{P2} \cdot \varepsilon_2 = F_{P1} \cdot \varepsilon_1 + (1 - F_{P1}) \cdot \varepsilon_2 \quad (53)$$

where  $\varepsilon$  is the observable enrichment factor in the reactant Q, and  $\varepsilon_i$ , as well as  $F_{Pi}$  are enrichment factor and yield of either transformation pathway, respectively. Such a case has the following consequences.

(i) When quantifying observable isotope fractionation, the contribution of either pathway must be understood, since the yield strongly influences the applicable  $\varepsilon$ .

(ii) In particular, care must be taken not to overlook a minor product with a large  $\varepsilon_i$  – otherwise a wrong mechanistic scenario would be constructed to explain an unrealistically high  $\varepsilon$ !

(iii) On the other hand, if the pathways are constrained and the pathway-dependent enrichment factors  $\varepsilon_i$  are well established, it is in principle possible to derive the contribution of either pathway from the magnitude of  $\varepsilon$ . This suggestion has been brought forward by van Breukelen<sup>142</sup> who extended it also to the interpretation of dual isotope slopes:

$$\frac{\Delta\delta^2\text{H}}{\Delta\delta^{13}\text{C}} \approx \frac{\varepsilon_{\text{H}}}{\varepsilon_{\text{C}}} \quad (17)$$

Although the concept is appealing, the possible presence of masking poses similar limits to such interpretations as to a general quantification of biotransformation. What if the  $\varepsilon_i$  of one pathway is masked in a field scenario, and the  $\varepsilon_i$  of the other not? The contribution of the first one would be greatly underestimated!

(iv) Finally, such interpretations may not even always be adequate. For example, chlorinated ethenes can be degraded abiotically at reactive surfaces such as of iron sulfides or zero-valent metals. This type of transformation gives primarily vicinal dichloroelimination products. It is reported to be associated with higher isotope fractionation than typically observed in biotransformations where hydrogenolysis products are formed.<sup>143,144</sup> Since two bonds are broken in dichloroelimination and only one in hydrogenolysis, the suggestion was brought forward that the magnitude of isotope fractionation in the reactant may reflect the type of product formation, similarly as expected for scenarios of Case A. Further it was suggested that this line of evidence can be used as an indicator to distinguish abiotic from biotic chlorinated ethene transformation from reactant data alone.<sup>143</sup> However, it cannot be excluded that the

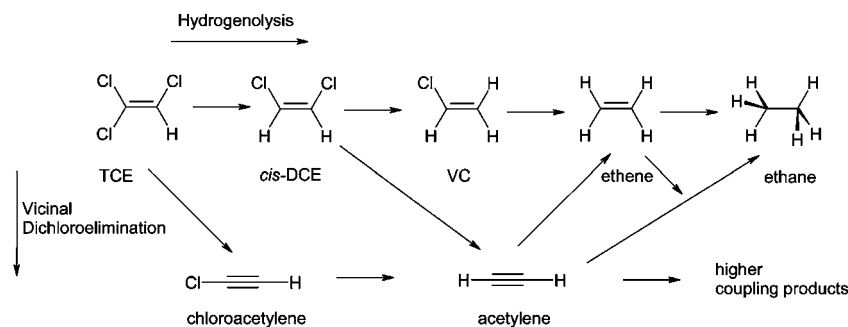
magnitude of fractionation is related to product formation in a more complicated manner, according to the possible scenario of case B.

**Case B.** The two product pathways share a common first irreversible step and a common intermediate. Subsequently the products are formed in parallel reactions with isotopic enrichment factors  $\varepsilon_I$  and  $\varepsilon_{II}$ . Like in the first case, isotope ratios of the two products differ by a constant value ( $\varepsilon_I - \varepsilon_{II}$ ). This time, however, it is the enrichment factor  $\varepsilon$  of the reactant that is constant, because it is uniquely given by the isotope effect of the first irreversible step. In contrast, the product-related enrichment factors vary as a function of product yield<sup>105</sup>

$$\varepsilon_{Q \rightarrow P1} = \varepsilon + (\varepsilon_I - \varepsilon_{II}) \cdot (1 - F_{P1}) \quad (54)$$

$$\varepsilon_{Q \rightarrow P2} = \varepsilon - (\varepsilon_I - \varepsilon_{II}) \cdot F_{P1} \quad (55)$$

The likelihood of either scenario was evaluated in chlorinated ethene transformation with different types of zero-valent iron<sup>94</sup> for which the following degradation pathways were determined.



Interpretations were complicated by the fact that different compounds were included in the comparison (TCE, *cis*-DCE, vinyl chloride), and that products may be formed in more than one way. Nonetheless, as predicted by both scenarios, product-related carbon isotopic enrichment factors showed a constant difference where the vicinal dichloroelimination product contained about 10‰ less <sup>13</sup>C than the hydrogenolysis product (Fig. 10). Although the product yield varied between 100% hydrogenolysis for vinyl chloride and 8% hydrogenolysis for TCE, Fig. 10 shows that observable enrichment factors  $\varepsilon$  fell within a rather narrow range, most of them clustering around -20‰. In contrast, it was the product-related enrichment factors which varied more strongly, with values for hydrogenolysis between  $\varepsilon_{VC \rightarrow \text{ethylene}} = -19.4\text{‰}$  and  $\varepsilon_{TCE \rightarrow \text{cis-DCE}} \approx -10\text{‰}$ .<sup>94</sup> As illustrated in Fig. 10, isotopic evidence therefore suggests that Case B prevailed and both products shared indeed a common irreversible step! Consequently, if the assumption of two different pathways was applied such as to distinguish abiotic and biotic transformation,<sup>143</sup> this would lead to inaccurate interpretations in the case of transformation by zero-valent iron.

This finding indicates that isotope analysis of reactants alone may not be sufficiently reliable to allow distinguishing abiotic and biotic chlorinated ethene degradation. At the same time, it indicates how such insight may potentially be obtained from isotope ratio measurements of reaction products.

The reason is that the same compounds are formed as sequential products in biotransformation, whereas they are formed as parallel products in abiotic transformation. Therefore, the evolution of isotope ratios over time is different for the two types of transformation, as shown in Fig. 9. In a very recent study, this line of evidence has made it possible to detect abiotic transformation by zero-valent iron treatment at a contaminated site where natural biodegradation was already going on!<sup>39</sup>

These examples show that isotope analysis of products can provide information about the steps involved in product formation, in a similar way as isotope fractionation of the reactant gives information about the first irreversible step. This potential for mechanistic elucidations has hardly been explored yet. For example, 1,1,2,2-tetrachloroethane reduction generates *cis*-DCE and *trans*-DCE as parallel products. Surprisingly, carbon isotope ratios of these products were found to differ by 2‰ in reaction with Cr(II), but not with zero-valent iron.<sup>145</sup> In a different study chloroethane and ethane were observed as parallel products of the transformation of 1,1-dichloroethane with zero-valent zinc. Although two C-Cl bonds are cleaved if

ethane is generated, but only one when chloroethane is formed, carbon isotope ratios of these products were identical!<sup>146</sup> Intriguing insight is therefore hidden in product isotope ratios, and novel mechanistic information can be expected if this source is explored in future studies.

## Outlook

Stable isotope fractionation measurements are at a point where applications to *monitor* contaminated sites have become mature,<sup>26</sup> but where the potential for a *mechanistic* process understanding is just beginning to unfold. Maybe most important in this context is the prospect to overcome an important current research gap: the possibility to transfer of insight from mechanistic laboratory studies to real-world systems.

**Bridging the gap to environmental processes.** Mechanistic studies in the laboratory typically approach the investigation of environmental transformations with model reactants that are designed to mimic enzymes or other natural catalysts. Mechanisms are frequently characterized through product studies, by linear free energy relationships (LFER) such as the Hammett relation, or by kinetic isotope effect studies with labelled substrate. While this approach can provide important insight into the model systems, the direct proof is generally missing that a model reactant adequately simulates processes in real-world systems. Stable isotope fractionation studies offer considerable



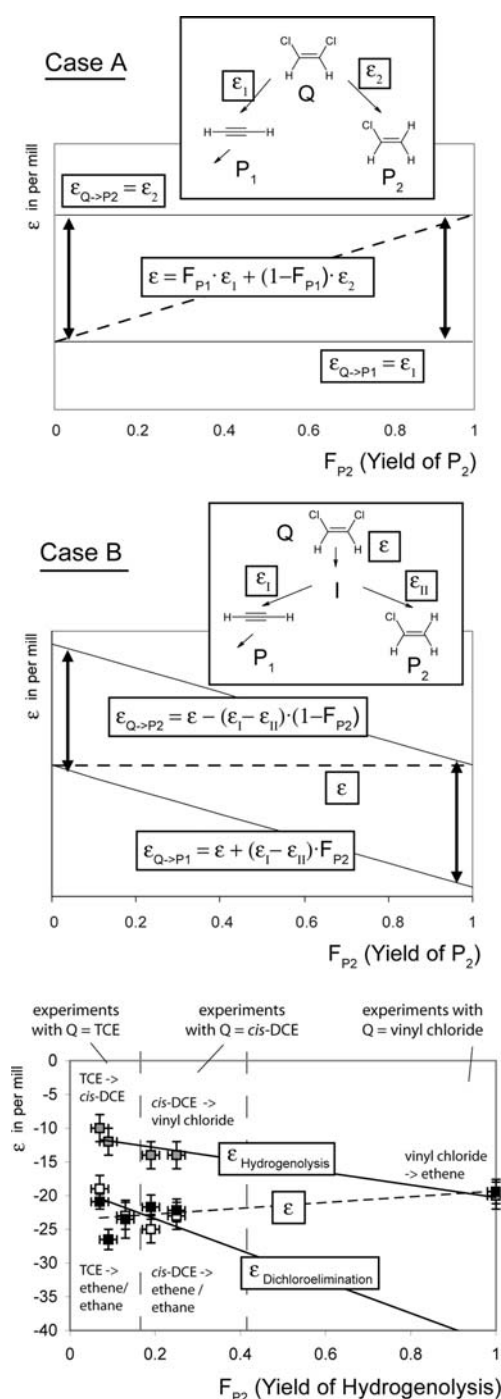


**Fig. 10** Isotopic enrichment factors in the reactant ( $\epsilon$ ) as well as between reactant and each product ( $\epsilon_{Q \rightarrow P_1}$ ,  $\epsilon_{Q \rightarrow P_2}$ ) depending on product yield in different scenarios of parallel product formation. Case A: two independent reactions occur in parallel. Case B: the parallel products share a common irreversible step with a common intermediate. Below, data is given from chlorinated ethylene degradation experiments with zero valent iron (ZVI).<sup>94</sup> Here, grey squares denote  $\epsilon_{Q \rightarrow \text{Hydrogenolysis Product}}$  data, white squares show  $\epsilon_{Q \rightarrow \text{Dichloroelimination Product}}$  data; both types of data were derived from differences in isotope values between reactant and respective product. In contrast, black squares denote  $\epsilon$  values obtained from reactant isotope data evaluated according to the Rayleigh equation. Lines are linear fits to either group of data points obtained in experiments with different chlorinated ethylenes and different types of ZVI.

potential to overcome this gap. As laid out in this review, changes in isotope values reflect information that may directly be related to the transition states of (bio)chemical reactions. Therefore, this method bears potential to provide a direct line of evidence that the same mechanism prevails in two different transformation reactions, for example by a model system in the laboratory, and through microorganisms at a contaminated site. In other words, mechanistic studies can become possible directly in environmental systems!

**Complementarity to product formation.** Information from stable isotope fractionation and product analysis is complementary. Isotope fractionation reflects transition states, whereas product analysis gives information about the outcome of a reaction. As discussed in this review, product analysis may even be essential for meaningful interpretations of observable isotope effects, and additional mechanistic information may be obtained if also product isotope ratios are analyzed. Therefore, best mechanistic insight is obtained when it is used in combination with product characterization and metabolite detection such as in a field study of aromatics degradation in a tar-oil contaminated aquifer.<sup>43</sup> Additional insight may even be obtained, if also the analysis of microbial communities and functional genes is included in the assessment.<sup>45,147,148</sup>

### Future challenges

**Conceptual understanding of multistep processes.** Mechanistic interpretations are challenged by the occurrence of multistep processes. How variable are observable enrichment factors  $\epsilon$ ? What information do they express? How can mechanistic interpretations be approached if one does not know which bottleneck is dominating? Based on the conceptual understanding summarized in this review, targeted approaches are needed to reduce this complexity. The isotope fractionation of selected reaction steps can potentially be de-masked through meaningful variation of transformation conditions such as pH or co-substrate concentration. Dual, or even triple<sup>88</sup> isotope studies may give information about different process steps. Finally, new concepts such as the link between isotope fractionation and bioavailability,<sup>127</sup> may aid in the identification of underlying principles.

**Accurate reference data.** As discussed in this review, mechanistic interpretations are currently limited by the need for accurate isotope effect reference data. Future mechanistic studies will, therefore, greatly profit from complementary computational calculations, as well as from isotope effect measurements with abiotic model reactants.

**Isotope analysis of new compounds.** Finally, most significant advances can be expected from improvement of analytical methods. Isotope studies with GC-IRMS have until now only been conducted with a limited number of environmental contaminants (see Table 1). If new target compounds are made amenable to compound-specific isotope analysis, a whole new field of applications can become possible, for example investigations of nitroaromatic compounds<sup>149</sup> or of diffuse contaminants such as pesticides.<sup>68,122,150</sup> To this end, a careful evaluation with respect to accuracy and precision is necessary,<sup>10,151</sup> optimization of the combustion process may be required<sup>68</sup> and non-volatile target compounds may have to be derivatized prior to isotope analysis.<sup>150</sup> Significant advances are also being made in

using LC-IRMS (liquid chromatography–isotope ratio mass spectrometry) to tackle compounds which are not amenable to GC-IRMS.<sup>168,169</sup> This approach avoids derivatization so that the analysis is easier to conduct and bias from additional carbon atoms is eliminated. On the downside, only carbon isotope analysis is presently possible, organic solvents must be strictly avoided and method quantification limits are a factor of ten higher.

**Isotope analysis of new elements.** In order to obtain mechanistic information from dual isotope slopes, isotope analysis must be feasible for more than one element. The majority of isotope studies, however, still analyses primarily carbon isotope fractionation. There is a need for isotope analysis of additional elements. Although nitrogen isotope analysis is routinely offered in commercial GC-IRMS setups, its accuracy and precision needs to be validated and optimized for new target compounds.<sup>68,149</sup> Also hydrogen isotope analysis is routinely possible for many target compounds, but remains problematic in chlorinated hydrocarbons because of HCl formation during pyrolysis to H<sub>2</sub>.<sup>152</sup> In contrast, chlorine isotope analysis in organic compounds has been pioneered in recent years<sup>4,132,133,153–155</sup> and is close to the point where it will routinely be used in transformation studies.<sup>90,156–159</sup>

**Fragment- and position-specific isotope analysis.** Finally, mechanistic isotope fractionation studies by GC-IRMS are limited by the fact that isotope effects can only be observed in the compound average rather than at specific molecular positions. Recently, the first studies have investigated the possibility of fragment-specific,<sup>122,160,161</sup> or even position-specific<sup>95</sup> isotope analysis of organic contaminants. Much improved insight can be expected from further advances in this direction.

In summary, the field of isotope fractionation investigations of natural contaminant degradation has expanded rapidly in recent years, and further advances are expected. A frequent selling argument for isotope fractionation measurements has been that it is often the only way to monitor and quantify the occurrence of natural transformation processes. This review makes a case for another strength of compound-specific isotope fractionation studies: they can become the most direct way to study (bio)chemical transformation mechanisms immediately in natural systems!

## References

- 1 J. T. Brenna, T. N. Corso, H. J. Tobias and R. J. Caimi, *Mass Spectrom. Rev.*, 1997, **16**, 227–258.
- 2 W. Meier-Augenstein, *J. Chromatogr. A*, 1999, **842**, 351–371.
- 3 A. L. Sessions, *J. Sep. Sci.*, 2006, **29**, 1946–1961.
- 4 O. Shouakar-Stash, S. K. Frape and R. J. Drimmie, *J. Contam. Hydrol.*, 2003, **60**, 211–228.
- 5 D. Hunkeler, N. Chollet, X. Pittet, R. Aravena, J. A. Cherry and B. L. Parker, *J. Contam. Hydrol.*, 2004, **74**, 265–282.
- 6 T. C. Schmidt, L. Zwank, M. Elsner, M. Berg, R. U. Meckenstock and S. B. Haderlein, *Anal. Bioanal. Chem.*, 2004, **378**, 283–300.
- 7 M. Blessing, T. C. Schmidt, R. Dinkel and S. B. Haderlein, *Environ. Sci. Technol.*, 2009, **43**, 2701–2707.
- 8 U.S. EPA, *Use of Monitored Natural Attenuation at Superfund, RCRA Corrective Action, and Underground Storage Tank Sites*, Office of Solid Waste and Emergency Response, 1999, Directive 9200.4–17P.
- 9 T. B. Coplen, J. K. Bohlke, P. De Bièvre, T. Ding, N. E. Holden, J. A. Hopple, H. R. Krouse, A. Lamberty, H. S. Peiser, K. Revesz, S. E. Rieder, K. J. R. Rosman, E. Roth, P. D. P. Taylor, R. D. Vocke and Y. K. Xiao, *Pure Appl. Chem.*, 2002, **74**, 1987–2017.
- 10 B. Sherwood Lollar, S. K. Hirschorn, M. M. G. Chartrand and G. Lacrampe Couloume, *Anal. Chem.*, 2007, **79**, 3469–3475.
- 11 T. B. Coplen, personal communication.
- 12 L. Melander and W. H. Saunders, *Reaction rates of isotopic molecules*, John Wiley, New York, 1980.
- 13 B. Sherwood Lollar, G. F. Slater, B. Sleep, M. Witt, G. M. Klecka, M. Harkness and J. Spivack, *Environ. Sci. Technol.*, 2001, **35**, 261–269.
- 14 D. Hunkeler and M. Elsner, in *Environmental Isotopes in Biodegradation and Bioremediation*, ed. C. M. Aelion, P. Hohener, D. Hunkeler and R. Aravena, CRC Press, Boca Raton, London, New York, 2010.
- 15 M. Elsner, J. McKelvie, G. Lacrampe Couloume and B. Sherwood Lollar, *Environ. Sci. Technol.*, 2007, **41**, 5693–5700.
- 16 E. M. LaBolle, G. E. Fogg, J. B. Eweis, J. Gravner and D. G. Leaist, *Water Resour. Res.*, 2008, **44**, W07405.
- 17 M. Rolle, G. Chiogna, R. Bauer, C. Griebler and P. Grathwohl, *Environ. Sci. Technol.*, 2010, **44**, 6167–6173.
- 18 F. D. Kopinke, A. Georgi, M. Voskamp and H. H. Richnow, *Environ. Sci. Technol.*, 2005, **39**, 6052–6062.
- 19 B. M. Van Breukelen and H. Prommer, *Environ. Sci. Technol.*, 2008, **42**, 2457–2463.
- 20 D. Bouchard, D. Hunkeler, P. Gaganis, R. Aravena, P. Hohener, M. M. Broholm and P. Kjeldsen, *Environ. Sci. Technol.*, 2008, **42**, 596–601.
- 21 T. Kuder, P. Philp and J. Allen, *Environ. Sci. Technol.*, 2009, **43**, 1763–1768.
- 22 J. W. S. Rayleigh, *Philos. Mag.*, 1896, **42**, 493–498.
- 23 J. Hoefs, in *Stable Isotope Geochemistry*, ed. P. J. Wyllie, Springer-Verlag, Chicago, 1987, pp. 1–25.
- 24 R. U. Meckenstock, B. Morasch, C. Griebler and H. H. Richnow, *J. Contam. Hydrol.*, 2004, **75**, 215–255.
- 25 M. Elsner, L. Zwank, D. Hunkeler and R. P. Schwarzenbach, *Environ. Sci. Technol.*, 2005, **39**, 6896–6916.
- 26 D. Hunkeler, R. U. Meckenstock, B. Sherwood Lollar, T. C. Schmidt and J. Wilson, *A Guide for Assessing Biodegradation and Source Identification of Organic Ground Water Contaminants using Compound Specific Isotope Analysis (CSIA)* PA 600/R-08/148 | December 2008 | www.epa.gov/ada, US EPA, Oklahoma, USA, 2008.
- 27 C. M. Aelion, P. Hohener, D. Hunkeler and R. Aravena, ed., *Environmental Isotopes in Bioremediation and Biodegradation*, CRC Press, 2010.
- 28 M. Thullner, H. H. Richnow and A. Fischer, in *Environmental and Regional Air Pollution*, ed. D. Gallo and R. Mancini, Nova Science Publishers, 2009.
- 29 T. Kuder, J. T. Wilson, P. Kaiser, R. Kolhatkar, P. Philp and J. Allen, *Environ. Sci. Technol.*, 2005, **39**, 213–220.
- 30 L. Zwank, M. Berg, M. Elsner, T. C. Schmidt, R. P. Schwarzenbach and S. B. Haderlein, *Environ. Sci. Technol.*, 2005, **39**, 1018–1029.
- 31 J. R. McKelvie, D. M. Mackay, N. R. de Sieyes, G. Lacrampe-Couloume and B. Sherwood Lollar, *J. Contam. Hydrol.*, 2007, **94**, 157–165.
- 32 L. E. Lesser, P. C. Johnson, R. Aravena, G. E. Spinnler, C. L. Bruce and J. P. Salanitro, *Environ. Sci. Technol.*, 2008, **42**, 6637–6643.
- 33 D. Hunkeler, R. Aravena and B. J. Butler, *Environ. Sci. Technol.*, 1999, **33**, 2733–2738.
- 34 M. G. Chartrand, A. Waller, T. E. Mattes, M. Elsner, G. Lacrampe-Couloume, J. M. Gossett, E. A. Edwards and B. Sherwood Lollar, *Environ. Sci. Technol.*, 2005, **39**, 1064–1070.
- 35 P. L. Morrill, G. Lacrampe-Couloume, G. F. Slater, B. E. Sleep, E. A. Edwards, M. L. McMaster, D. W. Major and B. Sherwood Lollar, *J. Contam. Hydrol.*, 2005, **76**, 279–293.
- 36 O. Atteia, M. Franceschi and A. Dupuy, *Environ. Sci. Technol.*, 2008, **42**, 3289–3295.
- 37 T. K. Kuhn, K. Hamonts, J. A. Dijk, H. Kalka, W. Stichler, D. Springael, W. Dejonghe and R. U. Meckenstock, *Environ. Sci. Technol.*, 2009, **43**, 5263–5269.
- 38 K. Hamonts, T. Kuhn, M. Maesen, J. Bronders, R. Lookman, H. Kalka, L. Diels, R. U. Meckenstock, D. Springael and W. Dejonghe, *Environ. Sci. Technol.*, 2009, **43**, 5270–5275.

- 39 M. Elsner, G. Lacrampe Couloume, S. A. Mancini, L. Burns and B. Sherwood Lollar, *Ground Water Monit. Remed.*, 2010, **30**, 79–95.
- 40 D. L. Song, M. E. Conrad, K. S. Sorenson and L. Alvarez-Cohen, *Environ. Sci. Technol.*, 2002, **36**, 2262–2268.
- 41 H. H. Richnow, E. Annweiler, W. Michaelis and R. U. Meckenstock, *J. Contam. Hydrol.*, 2003, **65**, 101–120.
- 42 H. H. Richnow, R. U. Meckenstock, L. A. Reitzel, A. Baun, A. Ledin and T. H. Christensen, *J. Contam. Hydrol.*, 2003, **64**, 59–72.
- 43 C. Griebler, M. Safinowski, A. Vieth, H. H. Richnow and R. U. Meckenstock, *Environ. Sci. Technol.*, 2004, **38**, 617–631.
- 44 A. Fischer, J. Bauer, R. U. Meckenstock, W. Stichler, C. Griebler, P. Maloszewski, M. Kastner and H. H. Richnow, *Environ. Sci. Technol.*, 2006, **40**, 4245–4252.
- 45 H. R. Beller, S. R. Kane, T. C. Legler, J. R. McKelvie, B. Sherwood Lollar, F. Pearson, L. Balser and D. M. Mackay, *Environ. Sci. Technol.*, 2008, **42**, 6065–6072.
- 46 P. Blum, D. Hunkeler, M. Weede, C. Beyer, P. Grathwohl and B. Morasch, *J. Contam. Hydrol.*, 2009, **105**, 118–130.
- 47 A. Bernstein, E. Adar, Z. Ronen, H. Lowag, W. Stichler and R. U. Meckenstock, *J. Contam. Hydrol.*, 2010, **111**, 25–35.
- 48 U.S. EPA, *Field Applications of In Situ Remediation Technologies: Permeable Reactive Barriers* EPA-68-W-00-084, U.S. Environmental Protection Agency, Office of Solid Waste and Emergency Response, Technology Innovation Office, Washington, DC, 2002.
- 49 H. Eisenmann and A. Fischer, in *Handbuch der Altlastensanierung und Flächenmanagement*, ed. V. Franzius, M. Altenbockum and T. Gerhold, Verlagsgruppe Hüthig Jehle Rehm, München, 2010.
- 50 F.-D. Kopinke, A. Georgi and H. H. Richnow, *Environ. Sci. Technol.*, 2005, **39**, 6052–6062.
- 51 A. Fischer, K. Theuerkorn, N. Stelzer, M. Gehre, M. Thullner and H. H. Richnow, *Environ. Sci. Technol.*, 2007, **41**, 3689–3696.
- 52 B. M. Van Breukelen, *Environ. Sci. Technol.*, 2007, **41**, 4980–4985.
- 53 Y. Abe and D. Hunkeler, *Environ. Sci. Technol.*, 2006, **40**, 1588–1596.
- 54 K. M. Salikhov, *Magnetic Isotope Effect in Radical Reactions*, Springer, Wien, New York, 1996.
- 55 Y. Q. Gao and R. A. Marcus, *Science*, 2001, **293**, 259–263.
- 56 A. E. Hartenbach, T. B. Hofstetter, P. R. Tentscher, S. Canonica, M. Berg and R. P. Schwarzenbach, *Environ. Sci. Technol.*, 2008, **42**, 7751–7756.
- 57 E. A. Schauble, *Geochim. Cosmochim. Acta*, 2007, **71**, 2170–2189.
- 58 J. G. Wiederhold, C. J. Cramer, K. Daniel, I. Infante, B. Bourdon and R. Kretzschmar, *Environ. Sci. Technol.*, 2010, **44**, 4191–4197.
- 59 A. Kohen and J. P. Klinman, *Chem. Biol.*, 1999, **6**, R191–R198.
- 60 S. R. Hartshorn and V. J. Shiner, *J. Am. Chem. Soc.*, 1972, **94**, 9002–9012.
- 61 D. M. Kiick, in *Enzyme Mechanism from Isotope Effects*, ed. P. F. Cook, CRC Press, Boca Raton, Ann Arbor, Boston, London, 1991, pp. 313–329.
- 62 D. A. Singleton and A. A. Thomas, *J. Am. Chem. Soc.*, 1995, **117**, 9357–9358.
- 63 P. F. Cook, *Enzyme mechanism from isotope effects*, CRC Press, 1991.
- 64 A. Kohen and H.-H. Limbach, *Isotope Effects in Chemistry and Biology*, CRC Press/Taylor and Francis, Boca Raton, FL, 2006.
- 65 M. Wolfsberg, W. A. Van Hook and P. Paneth, *Isotope Effects in the Chemical, Geological and Bio Sciences*, Springer, Dordrecht, Heidelberg, London, New York, 2010.
- 66 D. G. Truhlar, in *Isotope Effects in Chemistry and Biology*, ed. A. Kohen and H.-H. Limbach, CRC Press, Taylor and Francis, Boca Raton, 2006.
- 67 A. Dybala-Defratyka, L. Szatkowski, R. Kaminski, M. Wujec, A. Siwek and P. Paneth, *Environ. Sci. Technol.*, 2008, **42**, 7744–7750.
- 68 A. H. Meyer, H. Penning, H. Lowag and M. Elsner, *Environ. Sci. Technol.*, 2008, **42**, 7757–7763.
- 69 A. H. Meyer, H. Penning and M. Elsner, *Environ. Sci. Technol.*, 2009, **43**, 8079–8085.
- 70 D. Hunkeler and R. Aravena, *Appl. Environ. Microbiol.*, 2000, **66**, 4870–4876.
- 71 S. K. Hirschorn, M. J. Dinglasan, M. Elsner, S. A. Mancini, G. Lacrampe-Couloume, E. A. Edwards and B. Sherwood Lollar, *Geochim. Cosmochim. Acta*, 2004, **68**, A458–A458.
- 72 S. K. Hirschorn, M. J. Dinglasan, M. Elsner, S. A. Mancini, G. Lacrampe-Couloume, E. A. Edwards and B. Sherwood Lollar, *Environ. Sci. Technol.*, 2004, **38**, 4775–4781.
- 73 S. K. Hirschorn, M. J. Dinglasan-Panlilio, E. A. Edwards, G. Lacrampe-Couloume and B. Sherwood Lollar, *Environ. Microbiol.*, 2007, **9**, 1651–1657.
- 74 J. R. Gray, G. Lacrampe-Couloume, D. Gandhi, K. M. Scow, R. D. Wilson, D. M. Mackay and B. Sherwood Lollar, *Environ. Sci. Technol.*, 2002, **36**, 1931–1938.
- 75 D. Hunkeler, B. J. Butler, R. Aravena and J. F. Barker, *Environ. Sci. Technol.*, 2001, **35**, 676–681.
- 76 M. J. Whitticar, *Chem. Geol.*, 1999, **161**, 291–314.
- 77 R. Aravena and W. D. Robertson, *Ground Water*, 1998, **36**, 975–982.
- 78 B. Brunner, S. M. Bernasconi, J. Kleikemper and M. H. Schroth, *Geochim. Cosmochim. Acta*, 2005, **69**, 4773–4785.
- 79 A. Fischer, I. Herklotz, S. Herrmann, M. Thullner, S. A. B. Weelink, A. J. M. Stams, M. Schlömann, H. H. Richnow and C. Vogt, *Environ. Sci. Technol.*, 2008, **42**, 4356–4363.
- 80 S. A. Mancini, C. E. Devine, M. Elsner, M. E. Nandi, A. C. Ulrich, E. A. Edwards and B. Sherwood Lollar, *Environ. Sci. Technol.*, 2008, **42**, 8290–8296.
- 81 S. A. Mancini, S. K. Hirschorn, M. Elsner, G. Lacrampe-Couloume, B. E. Sleep, E. A. Edwards and B. Sherwood Lollar, *Environ. Sci. Technol.*, 2006, **40**, 7675–7681.
- 82 C. Vogt, E. Cyrus, I. Herklotz, D. Schlosser, A. Bahr, S. Herrmann, H. H. Richnow and A. Fischer, *Environ. Sci. Technol.*, 2008, **42**, 7793–7800.
- 83 N. B. Tobler, T. B. Hofstetter and R. P. Schwarzenbach, *Environ. Sci. Technol.*, 2008, **42**, 7786–7792.
- 84 T. B. Hofstetter, J. C. Spain, S. F. Nishino, J. Bolotin and R. P. Schwarzenbach, *Environ. Sci. Technol.*, 2008, **42**, 4764–4770.
- 85 A. Bernstein, Z. Ronen, E. Adar, R. Nativ, H. Lowag, W. Stichler and R. U. Meckenstock, *Environ. Sci. Technol.*, 2008, **42**, 7772–7777.
- 86 A. E. Hartenbach, T. B. Hofstetter, M. Aeschbacher, M. Sander, D. Kim, T. J. Strathmann, W. A. Arnold, C. J. Cramer and R. P. Schwarzenbach, *Environ. Sci. Technol.*, 2008, **42**, 8352–8359.
- 87 H. Penning, C. J. Cramer and M. Elsner, *Environ. Sci. Technol.*, 2008, **42**, 7764–7771.
- 88 H. Penning, S. R. Sorensen, A. H. Meyer, J. Aamand and M. Elsner, *Environ. Sci. Technol.*, 2010, **44**, 2372–2378.
- 89 Y. Abe, R. Aravena, J. Zopfi, O. Shouakar-Stash, E. Cox, J. D. Roberts and D. Hunkeler, *Environ. Sci. Technol.*, 2009, **43**, 101–107.
- 90 D. Hunkeler, B. M. Van Breukelen and M. Elsner, *Environ. Sci. Technol.*, 2009, **43**, 6750–6756.
- 91 M. Rosell, D. Barcelo, T. Rohwerder, U. Breuer, M. Gehre and H. H. Richnow, *Environ. Sci. Technol.*, 2007, **41**, 2036–2043.
- 92 J. R. McKelvie, M. R. Hyman, M. Elsner, C. Smith, D. M. Aslett, G. Lacrampe-Couloume and B. Sherwood Lollar, *Environ. Sci. Technol.*, 2009, **43**, 2793–2799.
- 93 M. Rosell, S. Finsterbusch, S. Jechalke, T. Hubschmann, C. Vogt and H. H. Richnow, *Environ. Sci. Technol.*, 2010, **44**, 309–315.
- 94 M. Elsner, M. Chartrand, N. VanStone, G. Lacrampe Couloume and B. Sherwood Lollar, *Environ. Sci. Technol.*, 2008, **42**, 5963–5970.
- 95 J. R. McKelvie, M. Elsner, A. J. Simpson, B. Sherwood Lollar and M. J. Simpson, *Environ. Sci. Technol.*, 2010, **44**, 1062–1068.
- 96 T. B. Hofstetter, A. Neumann, W. A. Arnold, A. Hartenbach, J. Bolotin, C. J. Cramer and R. P. Schwarzenbach, *Environ. Sci. Technol.*, 2008, **42**, 1997–2003.
- 97 Y. Abe, J. Zopfi and D. Hunkeler, *Isot. Environ. Health Stud.*, 2009, **45**, 18–26.
- 98 B. Morasch, H. H. Richnow, A. Vieth, B. Schink and R. U. Meckenstock, *Appl. Environ. Microbiol.*, 2004, **70**, 2935–2940.
- 99 D. A. Singleton and S. R. Merrigan, *J. Am. Chem. Soc.*, 2000, **122**, 11035–11036.
- 100 C. E. Rees, *Geochim. Cosmochim. Acta*, 1973, **37**, 1141–1162.
- 101 D. B. Northrop, *Biochemistry*, 1975, **14**, 2644–2651.
- 102 M. H. O’Leary, *BioScience*, 1988, **38**, 328–336.
- 103 M. H. O’Leary, *Annu. Rev. Biochem.*, 1989, **58**, 377–401.
- 104 G. D. Farquhar, J. R. Ehleringer and K. T. Hubick, *Annu. Rev. Plant Physiol. Plant Mol. Biol.*, 1989, **40**, 503–537.
- 105 J. M. Hayes, *Rev. Mineral. Geochem.*, 2001, **43**, 225–277.
- 106 M. W. Ruszczycky and V. E. Anderson, *J. Theor. Biol.*, 2006, **243**, 328–342.
- 107 J. F. Marlier, *Acc. Chem. Res.*, 2001, **34**, 283–290.



- 108 D. B. Northrop, *J. Chem. Educ.*, 1998, **75**, 1153–1157.
- 109 P. Paneth, *J. Mol. Struct.*, 1994, **321**, 35–44.
- 110 D. B. Northrop, *Annu. Rev. Biochem.*, 1981, **50**, 103–131.
- 111 W. W. Cleland, *Arch. Biochem. Biophys.*, 2005, **433**, 2–12.
- 112 M. Mungalo, R. U. Meckenstock, W. Stichler and F. Einsiedl, *Geochim. Cosmochim. Acta*, 2007, **71**, 4161–4171.
- 113 M. Mungalo, F. Einsiedl, R. U. Meckenstock and W. Stichler, *Geochim. Cosmochim. Acta*, 2008, **72**, 1513–1520.
- 114 F. Einsiedl, *Environ. Sci. Technol.*, 2009, **43**, 82–87.
- 115 I. Nijenhuis, J. Andert, K. Beck, M. Kastner, G. Diekert and H. H. Richnow, *Appl. Environ. Microbiol.*, 2005, **71**, 3413–3419.
- 116 D. Cichocka, M. Siegert, G. Imfeld, J. Andert, K. Beck, G. Diekert, H. H. Richnow and I. Nijenhuis, *FEMS Microbiol. Ecol.*, 2007, **62**, 98–107.
- 117 D. Cichocka, G. Imfeld, H. H. Richnow and I. Nijenhuis, *Chemosphere*, 2008, **71**, 639–648.
- 118 P. K. H. Lee, M. E. Conrad and L. Alvarez-Cohen, *Environ. Sci. Technol.*, 2007, **41**, 4277–4285.
- 119 I. J. T. Dinkla, E. M. Gabor and D. B. Janssen, *Appl. Environ. Microbiol.*, 2001, **67**, 3406–3412.
- 120 C. Aeppli, M. Berg, O. A. Cirpka, C. Holliger, R. P. Schwarzenbach and T. B. Hofstetter, *Environ. Sci. Technol.*, 2009, **43**, 8813–8820.
- 121 P. L. Morrill, B. E. Sleep, D. J. Seepersad, M. L. McMaster, E. D. Hood, C. LeBron, D. W. Major, E. A. Edwards and B. Sherwood Lollar, *J. Contam. Hydrol.*, 2009, **110**, 60–71.
- 122 H. Penning and M. Elsner, *Anal. Chem.*, 2007, **79**, 8399–8405.
- 123 H. Craig, *Geochim. Cosmochim. Acta*, 1953, **3**, 53–92.
- 124 J. F. Marlier, E. Campbell, C. Lai, M. Weber, L. A. Reinhardt and W. W. Cleland, *J. Org. Chem.*, 2006, **71**, 3829–3836.
- 125 L. Zwank, M. Elsner, A. Aeberhard, R. P. Schwarzenbach and S. B. Haderlein, *Environ. Sci. Technol.*, 2005, **39**, 5634–5641.
- 126 P. F. Cook, in *Enzyme mechanism from isotope effects*, ed. P. F. Cook, CRC Press, Boca Raton, FL, USA, Edition edn, 1991, pp. 231–245.
- 127 M. Thullner, M. Kampara, H. H. Richnow, H. Harms and L. Y. Wick, *Environ. Sci. Technol.*, 2008, **42**, 6544–6551.
- 128 M. Kampara, M. Thullner, H. H. Richnow, H. Harms and L. Y. Wick, *Environ. Sci. Technol.*, 2008, **42**, 6552–6558.
- 129 M. Kampara, M. Thullner, H. Harms and L. Y. Wick, *Appl. Microbiol. Biotechnol.*, 2009, **81**, 977–985.
- 130 T. N. P. Bosma, P. J. M. Middeldorp, G. Schraa and A. J. B. Zehnder, *Environ. Sci. Technol.*, 1997, **31**, 248–252.
- 131 H. L. Schmidt, *Naturwissenschaften*, 2003, **90**, 537–552.
- 132 C. M. Reddy, N. J. Drenzek, T. I. Eglinton, L. J. Heraty, N. C. Sturchio and V. J. Shiner, *Environ. Sci. Pollut. Res.*, 2002, **9**, 183–186.
- 133 H. Holmstrand, M. Mandalakis, Z. Zencak, P. Andersson and O. Gustafsson, *Chemosphere*, 2007, **69**, 1533–1539.
- 134 J. R. McKelvie, M. R. Hyman, M. Elsner, C. Smith, D. M. Aslett, G. Lacrampe-Couloume and B. Sherwood Lollar, *Environ. Sci. Technol.*, 2009, **43**, 2793–2799.
- 135 T. C. Schmidt, M. Schirmer, H. Weiss and S. B. Haderlein, *J. Contam. Hydrol.*, 2004, **70**, 173–203.
- 136 D. Hunkeler, R. Aravena and E. Cox, *Environ. Sci. Technol.*, 2002, **36**, 3378–3384.
- 137 G. F. Slater, B. Sherwood Lollar, B. E. Sleep and E. A. Edwards, *Environ. Sci. Technol.*, 2001, **35**, 901–907.
- 138 Y. Bloom, R. Aravena, D. Hunkeler, E. Edwards and S. K. Frape, *Environ. Sci. Technol.*, 2000, **34**, 2768–2772.
- 139 B. M. Van Breukelen, D. Hunkeler and F. Volkerling, *Environ. Sci. Technol.*, 2005, **39**, 4189–4197.
- 140 C. Aeppli, T. B. Hofstetter, H. I. F. Amaral, R. Kipfer, R. P. Schwarzenbach and M. Berg, *Environ. Sci. Technol.*, 2010, **44**, 3705–3711.
- 141 M. Blessing, M. Jochmann and T. Schmidt, *Anal. Bioanal. Chem.*, 2008, **390**, 591–603.
- 142 B. M. Van Breukelen, *Environ. Sci. Technol.*, 2007, **41**, 4004–4010.
- 143 X. Liang, Y. Dong, T. Kuder, L. R. Krumholz, R. P. Philp and E. C. Butler, *Environ. Sci. Technol.*, 2007, **41**, 7094–7100.
- 144 X. Liang, R. Paul Philp and E. C. Butler, *Chemosphere*, 2009, **75**, 63–69.
- 145 M. Elsner, D. M. Cwiertny, A. L. Roberts and B. Sherwood Lollar, *Environ. Sci. Technol.*, 2007, **41**, 4111–4117.
- 146 N. VanStone, M. Elsner, G. Lacrampe-Couloume, S. Mabury and B. Sherwood Lollar, *Environ. Sci. Technol.*, 2008, **42**, 126–132.
- 147 J. R. McKelvie, S. K. Hirschorn, G. Lacrampe-Couloume, J. Lindstrom, J. Braddock, K. Finneran, D. Trego and B. Sherwood Lollar, *Ground Water Monit. Rem.*, 2007, **27**, 63–73.
- 148 G. Imfeld, C. E. Aragones, I. Fetzer, E. Meszaros, S. Zeiger, I. Nijenhuis, M. Nikolausz, S. Delerce and H. H. Richnow, *FEMS Microbiol. Ecol.*, 2010, **72**, 74–88.
- 149 M. Berg, J. Bolotin and T. B. Hofstetter, *Anal. Chem.*, 2007, **79**, 2386–2393.
- 150 S. Reinicke, A. Bernstein and M. Elsner, *Anal. Chem.*, 2010, **82**, 2013–2019.
- 151 M. A. Jochmann, M. Blessing, S. B. Haderlein and T. C. Schmidt, *Rapid Commun. Mass Spectrom.*, 2006, **20**, 3639–3648.
- 152 M. M. G. Chartrand, S. K. Hirschorn, G. Lacrampe-Couloume and B. Sherwood Lollar, *Rapid Commun. Mass Spectrom.*, 2007, **21**, 1841–1847.
- 153 C. M. Reddy, L. Xu, N. J. Drenzek, N. C. Sturchio, L. J. Heraty, C. Kimblin and A. Butler, *J. Am. Chem. Soc.*, 2002, **124**, 14526–14527.
- 154 T. B. Hofstetter, C. M. Reddy, L. J. Heraty, M. Berg and N. C. Sturchio, *Environ. Sci. Technol.*, 2007, **41**, 4662–4668.
- 155 H. Holmstrand, P. Andersson and O. Gustafsson, *Anal. Chem.*, 2004, **76**, 2336–2342.
- 156 O. Shouakar-Stash, R. J. Drimmie, M. Zhang and S. K. Frape, *Appl. Geochem.*, 2006, **21**, 766–781.
- 157 K. Sakaguchi-Soder, J. Jager, H. Grund, F. Matthaues and C. Schuth, *Rapid Commun. Mass Spectrom.*, 2007, **21**, 3077–3084.
- 158 M. Elsner and D. Hunkeler, *Anal. Chem.*, 2008, **80**, 4731–4740.
- 159 C. Aeppli, H. Holmstrand, P. Andersson and O. Gustafsson, *Anal. Chem.*, 2010, **82**, 420–426.
- 160 J. T. Brenna, *Rapid Commun. Mass Spectrom.*, 2001, **15**, 1252–1262.
- 161 C. Gauchotte, G. O'Sullivan, D. Simon and R. M. Kalin, *Rapid Commun. Mass Spectrom.*, 2009, **23**, 3183–3193.
- 162 D. Hunkeler, N. Andersen, R. Aravena, S. M. Bernasconi and B. J. Butler, *Environ. Sci. Technol.*, 2001, **35**, 3462–3467.
- 163 S. A. Mancini, A. C. Ulrich, G. Lacrampe-Couloume, B. Sleep, E. A. Edwards and B. Sherwood Lollar, *Appl. Environ. Microbiol.*, 2003, **69**, 191–198.
- 164 J. A. M. Ward, J. M. E. Ahad, G. Lacrampe-Couloume, G. F. Slater, E. A. Edwards and B. Sherwood Lollar, *Environ. Sci. Technol.*, 2000, **34**, 4577–4581.
- 165 B. Morasch, H. H. Richnow, B. Schink and R. U. Meckenstock, *Appl. Environ. Microbiol.*, 2001, **67**, 4842–4849.
- 166 B. Morasch, H. H. Richnow, B. Schink, A. Vieth and R. U. Meckenstock, *Appl. Environ. Microbiol.*, 2002, **68**, 5191–5194.
- 167 N. B. Tobler, T. B. Hofstetter and R. P. Schwarzenbach, *Environ. Sci. Technol.*, 2007, **41**, 7773–7780.
- 168 M. Krummen, A. W. Hilkert, D. Juchelka, A. Duhr, H. J. Schluter and R. Pesch, *Rapid Commun. Mass Spectrom.*, 2004, **18**, 2260–2266.
- 169 J. P. Godin, J. Hau, L. B. Fay and G. Hopfgartner, *Rapid Commun. Mass Spectrom.*, 2005, **19**, 2689–2698.